# Micromechanical modeling of stress-induced phase transformations. Part 1. Thermodynamics and kinetics of coupled interface propagation and reorientation

Valery I. Levitas [a,b,*], Istemi B. Ozsoy [b,c]

[a] *Iowa State University, Departments of Mechanical Engineering, Aerospace Engineering and Material Science and Engineering, Ames, Iowa 50011, USA*
[b] *Texas Tech University, Department of Mechanical Engineering, Lubbock, TX 79409, USA*
[c] *TOBB University of Economics and Technology, Department of Mechanical Engineering, Ankara, 06560, Turkey*

## Abstract

The universal (i.e. independent of the constitutive equations) thermodynamic driving force for coherent interface reorientation during first-order phase transformations in solids is derived for small and finite strains. The derivation is performed for a representative volume with plane interfaces, homogeneous stresses and strains in phases and macroscopically homogeneous boundary conditions. Dissipation function for coupled interface (or multiple parallel interfaces) reorientation and propagation is derived for combined athermal and drag interface friction. The relation between the rates of single and multiple interface reorientation and propagation and the corresponding driving forces are derived using extremum principles of irreversible thermodynamics. They are used to derive complete system of equations for evolution of martensitic microstructure (consisting of austenite and a fine mixture of two martensitic variants) in a representative volume under complex thermomechanical loading. Viscous dissipation at the interface level introduces size dependence in the kinetic equation for the rate of volume fraction. General relationships for a representative volume with moving interfaces under piece-wise homogeneous boundary conditions are derived. It was found that the driving force for interface reorientation appears when macroscopically homogeneous stress or strain are prescribed, which corresponds to experiments. Boundary conditions are satisfied in an averaged way. In Part 2 of the paper [Levitas, V.I., Ozsoy, I.B., 2008. Micromechanical modeling of stress-

---

* Corresponding author. Tel.: +1 806 742 3563x244; fax: +1 806 742 3540.
  *E-mail address:* valery.levitas@ttu.edu (V.I. Levitas).

induced phase transformations. Part 2. Computational algorithms and examples. Int. J. Plasticity (2008)], the developed theory is applied to the numerical modeling of the evolution of martensitic microstructure under three-dimensional thermomechanical loading during cubic-tetragonal and tetragonal-orthorhombic phase transformations.

## 1. Introduction

Solid–solid phase transformations are widely studied in physical experiments. They are used in modern technologies and broadly spread in nature. We will focus on displacive phase transformations that are dominated by the deformation of a unit crystal cell that is described by transformation (Bain) strain tensor $\varepsilon_t$. They include martensitic phase transformations during which atoms do not change their neighbors, and reconstructive phase transformations in opposite case. For both of them, we will neglect any intra-cell displacements or shuffles since stresses do not produce work on them. Even in the cases when shuffles are responsible for lattice instability and initiation of phase transformation, we assume in our thermodynamic approach that they are expressed in terms of $\varepsilon_t$ by energy minimization (Salje, 1990). This is the usual way of thermodynamic study of reconstructive fcc–bcc and fcc–hcp in ferrous alloys (Olson and Cohen, 1972). Martensitic phase transformations represent the main deformation mechanism of shape memory alloys (SMA) and cause pseudoelasticity and pseudoplasticity phenomena, as well as one- and two-ways shape memory effects. We will neglect dislocation plasticity and consider coherent interfaces only for which displacements are continuous across the interface. Martensitic transformations, for example, in shape memory alloys, ceramics and steels, produce specific sophisticated multi-connected microstructure. This microstructure determines the mechanical and generally physical properties of the material, internal stresses, and possible engineering applications. As stated in Olson (1997), one of the goals of computational material design is the formation of a desired microstructure based on chosen criteria.

Due to symmetry of crystal lattice, there is a finite number (e.g. 12 for the phase transformation from a cubic to monoclinic lattice) of crystallographically equivalent martensitic variants $M_i$. Each martensitic variant has the same components of the transformation strain tensor $\varepsilon_{ti}$, but in its own crystallographic basis. Each martensitic unit (for example, plate or lath) usually represents a fine mixture of several martensitic variants that lead to the reduction of elastic energy of internal stresses. Each grain of polycrystalline material or single crystal is filled by numerous martensitic units. Consequently, study of the evolution of microstructures during solid–solid phase transformation is a complex multiscale problem.

At nanoscale, Ginzburg–Landau, or phase field approach, is used to model the microstructure evolution Artemev et al. (2000, 2001), Saxena et al. (1997), Rasmussen et al. (2001), Wang and Khachaturyan (1997), and Chen (2002). Recently (Levitas and Lee, 2007), an athermal threshold was introduced in a phase field approach. However, it is mentioned in Levitas et al. (2004) and Idesman et al. (2005) that since it resolves each martensitic variant (characteristic width is 10 nm) and each interface (characteristic size is

1 nm), maximum size of the sample that can be treated numerically does not exceed 100–1000 nm. Recently (Levitas et al., 2004; Idesman et al., 2005), we developed a mesoscale phase field approach that allows us to model stress-induced martensitic microstructure in sample of size greater than 100 nm, and without an upper limit. The main idea was that when internal stresses are taken into account, macroscopic stress–strain relationships exhibit strain softening. Strain softening leads to transformation strain localization in some regions that are martensitic units. In such a way, discrete martensitic microstructure is reproduced as a result of the solution of a boundary-value problem without any effort to track interfaces. However, the micromechanical models in those papers were very simplified. One of the goals of the current paper is to develop an advanced micromechanical model that can be used in a finite element simulation of discrete martensitic microstructures in a macroscopic sample. This model has to reproduce all crystallographic and microstructural characteristics, like orientation of the interfaces between austenite and martensite and between martensitic variants, and volume fraction of austenite and martensitic variants and their evolution under prescribed complex three-dimensional thermomechanical loading.

We will consider several types of representative volumes (Fig. 1) in which two phases (we will call them austenite and martensite, but our treatment is not limited to martensitic transformations) are divided by a parallel interface or multiple parallel interfaces. Martensite itself may consist of a fine mixture of two alternating martensitic variants with parallel interfaces. Such a multi-layered system was considered in many publications, starting with pioneering work by Roitburd (1974, 1993), Khachaturyan and Shatalov (1969) and Khachaturyan (1983). Before them, the main crystallographic parameters of martensitic microstructure has been determined on the basis on geometrically nonlinear
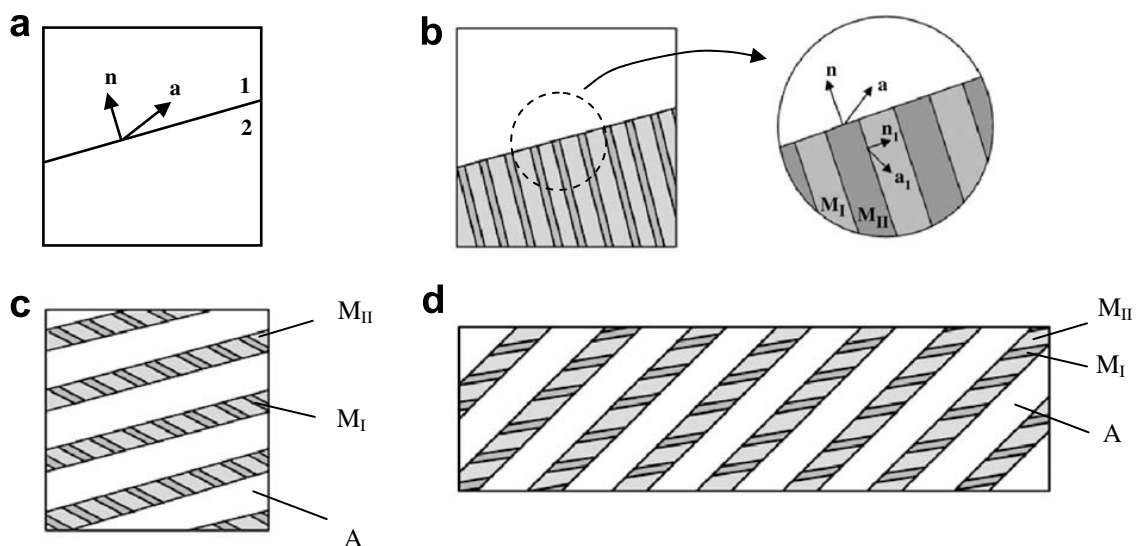


Fig. 1. Several types of representative volumes treated in this paper: (a) Single plane interface between phases 1 and 2 (or between austenite and martensite); (b) Single plane interface between austenite and martensite when martensite consists of alternating martensitic variants $M_I$ and $M_{II}$. (c) and (d) Multiple martensitic units consisting of alternating martensitic variants $M_I$ and $M_{II}$ separated by plane interfaces from austenite. In (d) parallelepiped is significantly elongated along one of the sides, so the majority of interfaces between austenite and martensite are equal. Each martensitic plate in (c) and (d) can be considered as a representative parallelepiped for alternating martensitic variants $M_I$ and $M_{II}$.

crystallographic theory, Wechsler et al. (1953) and Wayman (1964). One of the main problems of the crystallographic theory of martensite is to find for a given transformation strain, the structure and orientation of the A–M interface. Namely, one has to find lattice invariant shear due to slip or twinning, the rotation of the crystal lattice and the normal to the A–M interface which produces an undeformable (invariant) plane. Along this habit plane the compatibility condition between M and rigid A is fulfilled. Since the theory contains no principle whereby the single or multiple shear systems are selected, they have to be assumed and evaluated by comparison with experiments. To describe some experiments, one has to assume isotropic or anisotropic dilatation of the interface as a fitting parameter because of the elastoplastic deformation of A. This theory is a purely geometric one without any stresses. Nevertheless, the theory describes well a lot of experiments.

The mathematical theory of martensitic microstructure formation (Ball and James, 1987; Kohn, 1991; Bhattacharya, 2004) derives the main crystallographic characteristics from the energy minimization principle for elastic materials at finite strains. As the global minimum of energy corresponds to a stress-free configuration, the problem again reduces to the geometric one. Slip is not considered in this theory. For an A–M interface and a combination of two martensitic variants (which are in twin relation) in proper proportion, the normals to the interfaces between the variants and between A and M are found. This result is equivalent to crystallographic theory in Wayman (1964). However, this more strict and general approach did not require guessing of shear system and gave a number of new results.

The geometrically linear theory of martensitic phase transformation in elastic materials by Roitburd (1974, 1993), Khachaturyan (1983) and Roytburd and Slutsker (2001) is based on energy minimization as well. However, it was also applied to the cases where crystallographic parameters depend on external stresses and internal stresses being present. These approaches, however, neglect an athermal threshold to interface propagation that is caused by interaction between the moving interface and the long-range stress fields of defects (point defects, dislocations, grain and subgrain boundaries), as well as the Peierls barrier and acoustic emission. The athermal friction is similar to dry friction in contact problems, and causes dissipation even at infinitesimal interface velocity. In the presence of the athermal friction, microstructure evolution is not governed by energy minimization, and incremental problem formulation (similar to plasticity) is required. The mathematical approach to such problems was initiated by Mielke et al. (2002) based on the postulate of realizability (Levitas, 1995, 1998, 2000), and further developed in Kruzik et al. (2005). Aspects of modeling martensite–martensite transformation can be found in particular in Sun and Hwang (1993), Marketz and Fischer (1996), Levitas and Stein (1997), Zheng and Liu (2002), Liu and Xie (2003), Thamburaja (2005), Pan et al. (2007), Popov and Lagoudas (2007), Auricchio et al. (2007), Hall et al. (2007), Shaw (2000), Muller and Bruhns (2006) and Gao et al. (2000).

Stupkiewicz and Petryk (2002) studied stress-induced evolution of the laminated austenite–martensite microstructure with allowing for athermal interface friction. Internal twinned structure of martensite was determined based on crystallographic theory and did not evolve, which is easy to change. However, interface reorientation (i.e. rotation of the normal to the interface) was not taken into account.

Our starting point in this paper is a consideration of thermodynamics and the kinetics of interface propagation and reorientation in the representative volumes shown in Fig. 1. Homogeneous stresses and strains in phases are assumed and boundary conditions are met in an averaged way (see Eqs. (1) and (2)). The universal (independent of specific constitu-

tive relations) thermodynamic driving force for interface propagation during solid–solid phase transformation, the celebrated Eshelby driving force, Eshelby (1970), Kaganova and Roitburd (1988), Abeyaratne and Knowles (1993) and its generalization in the form of the tensor of chemical potential, Grinfeld (1991), have been known for decades. In marked contrast, the universal driving force for interface rotation has not been previously obtained. Orientation of an interface for linear elastic solids when it does not coincide with an invariant plane (i.e. when internal stresses are generated) and changes in its orientation under uniaxial external stress was studied in Pankova and Roytburd (1984), Roitburd and Kosenko (1976, 1977), Roitburd (1983), and Roytburd and Slutsker (1997, 2001) using energy minimization. Despite the significant progress, these methods explore specific expressions for elastic energy of the mixture of two linearly elastic phases when they are relatively simple, and are difficult to expand for more sophisticated transformation strains, elastic anisotropy, nonlinear elasticity, finite strains, and complex loading. Energy minimization cannot be used for those practically important cases where athermal interface friction is significant.

This paper contains several new results. First, an explicit universal (i.e. independent of specific constitutive relations) expression for the thermodynamic driving force for interface rotation is derived for small and finite strains. Second, we derive an explicit expression for the dissipation rate for simultaneous interface propagation and interface rotation that takes into account both athermal and drag interface friction for single and multiple interfaces. For athermal friction, two separate cases are treated when the center of interface rotation belongs or does not belong to the interface. Limit curve in the plane of driving forces for interface propagation and rotation is derived within which the interface motion is impossible. The counterpart of the associated flow (or phase transformation) rule is formulated. Relationships between driving forces for interface propagation and rotation and rates of interface propagation and rotation are derived using the extremum principles of irreversible thermodynamics separately for athermal and viscous interface friction. Explicit inverse relationships between the rates of interface rotation and interface propagation, and the driving forces for interface rotation and interface propagation are obtained using Legendre transformation. For viscous friction, the interface propagation and rotation are independent of each other, whereas athermal friction introduces a nontrivial coupling between them. In particular, during slow interface propagation, even an infinitesimal driving force for interface rotation causes a finite interface rotation rate. For multiple interfaces, the following problem arose: when varying the ratio of interface propagation to rotation rate, the number of interfaces, for which the center of the interface rotation belongs or does not belong to the interface, vary discontinuously, and for each interval, separate equations have to be used. However, we found that even for this case, dissipation function and relationships between thermodynamic forces and conjugate rate are continuous. Using separate equation for multiple intervals is not effective in numerical calculations. A simple and accurate single-function approximation of these equations was found in the paper. It was also found that viscous dissipation at the interface level (that was not considered in previous publications on phase transitions in laminated structures) introduces size dependence in the kinetic equation for the rate of volume fraction. Thermodynamic driving forces for interface orientation and propagation and stresses in each phase are found for the austenite–martensite system when martensite consists of alternating martensite I–martensite II variants. Thus, internal evolution of the martensitic unit is included as well.

In the previous work on micro to macro transition for laminated structures with phase transformations (Khachaturyan, 1983; Roytburd and Slutsker, 2001; Stupkiewicz and Petryk (2002)) boundary conditions have not been treated. In the general study of micro to macro transition (Hill, 1984), tractions corresponding to a constant stress tensor or displacements corresponding to a constant deformation gradient (i.e. macroscopically homogeneous boundary conditions) are applied to prove transfer of important energetic relationships. Here, we studied also a more general case of macroscopically piece-wise homogeneous boundary conditions different for boundaries corresponding to different phases. We found that the driving force for interface reorientation appears when macroscopically homogeneous stress or strain are prescribed and does not appear for piece-wise homogeneous boundary conditions. Since all experiments are performed under prescribed macroscopically homogeneous boundary conditions (see e.g. Abeyaratne et al., 1996), we use them (similar to all known studies of representative volumes in Fig. 1). There is well-known contradiction between assumption of piece-wise homogeneous stresses and strains in phases and homogeneous boundary conditions. Homogeneous stresses and strains in phases are a strong assumption which is used in order to perform analytical treatment of the problem and because in most cases it is fulfilled in the major part of the volume away from boundary and some transition layers (see e.g. Abeyaratne et al., 1996; Bhattacharya, 2004). Boundary conditions are met in averaged sense (see Eqs. (1) and (2)), which is well-known approximation. It works well e.g. for fine layered microstructure. In Part 2 of the paper (Levitas and Ozsoy, 2008), the developed theory is applied to numerical modeling of the evolution of martensitic microstructure under three-dimensional thermomechanical loading during cubic-tetragonal and tetragonal-orthorhombic phase transformations. Some preliminary results are published in Levitas (2002) and Levitas et al. (2007).

The paper is organized as follows. In Section 2, the driving force for an interface orientation is derived and analyzed for small strains. In Section 3, expression for dissipation rate and kinetic equations for interface reorientation and propagation are derived for single and multiple interfaces. In Section 4, equations for stresses and strains in phases are derived. Thermodynamic driving forces for interface orientation and propagation are found for the case austenite–martensite system when martensite consists of alternating martensite I–martensite II variants. In Section 5, interface orientation and internal structure of embryo is considered. Thermodynamic driving force for interface reorientation for finite strains is derived in Section 6. Micro to macro transition for representative volume with moving interfaces under macroscopically homogeneous and piece-wise homogeneous boundary conditions is studied in Section 7. Section 8 contains concluding remarks. Direct tensor notations are use throughout the paper. Vectors and tensors are designated by boldface letters; $\cdot$ and $:$ designates contraction of tensors or vectors over one or two nearest indexes; $A^{\text{t}}$ and $\dot{A}$ designate transposed tensor $A$ and material time derivative, $(A)_s$ means symmetrization and $[A] = A_2 - A_1$ is the jump of a tensor across an interface.

## 2. Universal thermodynamic driving forces for interface propagation and reorientation

We consider a rectangular parallelepiped $V$ containing two phases, 1 and 2, divided by a plane interface $\Sigma$ (or parallel interfaces) with the unit normal $\boldsymbol{n}$ directed toward phase 1 (Fig. 1a), under external stresses $\boldsymbol{\sigma}$. Let $\boldsymbol{\varepsilon}_i$ and $\boldsymbol{\sigma}_i$ be the constant strain and stress tensors in each phase. Then

$$\varepsilon = c_1\varepsilon_1 + c_2\varepsilon_2, \tag{1}$$

$$\sigma = c_1\sigma_1 + c_2\sigma_2, \tag{2}$$

$$\psi = c_1\psi_1(\varepsilon_1,\theta) + c_2\psi_2(\varepsilon_2,\theta), \quad s = c_1 s_1(\varepsilon_1,\theta) + c_2 s_2(\varepsilon_2,\theta) \tag{3}$$

are the strain and stress tensors, as well as the Helmholtz free energy and entropy, both per unit volume, averaged over $V$. Here $c_i$ is the volume fraction of the $i$th phase ($c = c_2 = 1 - c_1$) and $\theta$ is the temperature homogeneous in $V$. As is usual for strain-dominated phase transformations with coherent interfaces (for which displacements are continuous across an interface), we neglect the interface energy in comparison to the elastic energy. It follows from the thermodynamics of each phase that:

$$\sigma_1 = \frac{\partial\psi_1}{\partial\varepsilon_1}, \quad \sigma_2 = \frac{\partial\psi_2}{\partial\varepsilon_2} \tag{4}$$

and

$$s_1 = -\frac{\partial\psi_1}{\partial\theta}, \quad s_2 = -\frac{\partial\psi_2}{\partial\theta}. \tag{5}$$

The dissipation rate per unit volume is

$$D_V = \sigma : \dot{\varepsilon} - \dot{\psi} - s\dot{\theta} \geqslant 0. \tag{6}$$

Since $\dot{\psi} = c_1(\partial\psi_1/\partial\varepsilon_1)\dot{\varepsilon}_1 + c_2(\partial\psi_2/\partial\varepsilon_2)\dot{\varepsilon}_2 + c_1(\partial\psi_1/\partial\theta)\dot{\theta} + c_2(\partial\psi_2/\partial\theta)\dot{\theta} + \dot{c}_1\psi_1 + \dot{c}_2\psi_2$ and $\dot{c}_1 = -\dot{c}_2 = -\dot{c}$, we have $\dot{\psi} = c_1\sigma_1 : \dot{\varepsilon}_1 + c_2\sigma_2 : \dot{\varepsilon}_2 - (c_1 s_1\dot{\theta} + c_2 s_2\dot{\theta}) + [\psi]\dot{c}$ and $\dot{\varepsilon} = c_1\dot{\varepsilon}_1 + c_2\dot{\varepsilon}_2 + [\varepsilon]\dot{c}$.

Inserting in $D_V$ the expressions for $\dot{\varepsilon}$ and $\dot{\psi}$, we obtain

$$D_V = X_c\dot{c} + c_1(\sigma - \sigma_1) : \dot{\varepsilon}_1 + + c_2(\sigma - \sigma_2) : \dot{\varepsilon}_2 \geqslant 0, \tag{7}$$

where $X_c := \sigma : [\varepsilon] - [\psi]$ is the Eshelby driving force for interface propagation during the phase transformation $1 \leftrightarrow 2$. Let us simplify the two last terms in Eq. (7). Using $\sigma = (1-c)\sigma_1 + c\sigma_2$, we obtain $\sigma - \sigma_1 = c[\sigma]$, $\sigma - \sigma_2 = (c-1)[\sigma]$ and

$$c_1(\sigma - \sigma_1) : \dot{\varepsilon}_1 + c_2(\sigma - \sigma_2) : \dot{\varepsilon}_2 = -c_1 c_2[\sigma] : (\dot{\varepsilon}_2 - \dot{\varepsilon}_1) = -c_1 c_2[\sigma] : [\dot{\varepsilon}]. \tag{8}$$

Using the Hadamard compatibility condition and the traction continuity condition

$$[\varepsilon] = (\boldsymbol{an})_s, \quad [\sigma] \cdot \boldsymbol{n} = 0, \tag{9}$$

where the vector $\boldsymbol{a}$ characterizes the strain jump, Eq. (8) can be further transformed to

$$-c_1 c_2[\sigma] : [\dot{\varepsilon}] = -c_1 c_2[\sigma] : (\dot{\boldsymbol{n}}\boldsymbol{a} + \boldsymbol{n}\dot{\boldsymbol{a}}) = -c_1 c_2[\sigma] : \dot{\boldsymbol{n}}\boldsymbol{a} = -c_1 c_2\boldsymbol{a} \cdot [\sigma] \cdot \dot{\boldsymbol{n}}. \tag{10}$$

Thus, the rate of dissipation (7) can be presented in the form

$$D_V = X_c\dot{c} + \boldsymbol{X}_n \cdot \dot{\boldsymbol{n}} \geqslant 0, \tag{11}$$

where

$$\boldsymbol{X}_n := -c_1 c_2\boldsymbol{a} \cdot [\sigma] \tag{12}$$

is the expression for the universal thermodynamic driving force for interface rotation.

Decomposing $\boldsymbol{a} = a_n\boldsymbol{n} + \boldsymbol{a}_\tau$, where $a_n\boldsymbol{n}$ and $\boldsymbol{a}_\tau$ are collinear and orthogonal to $\boldsymbol{n}$ (Fig. 2), and using $\boldsymbol{n} \cdot [\sigma] = 0$, we obtain

$$\boldsymbol{X}_n = -c_1 c_2\boldsymbol{a}_\tau \cdot [\sigma]. \tag{13}$$
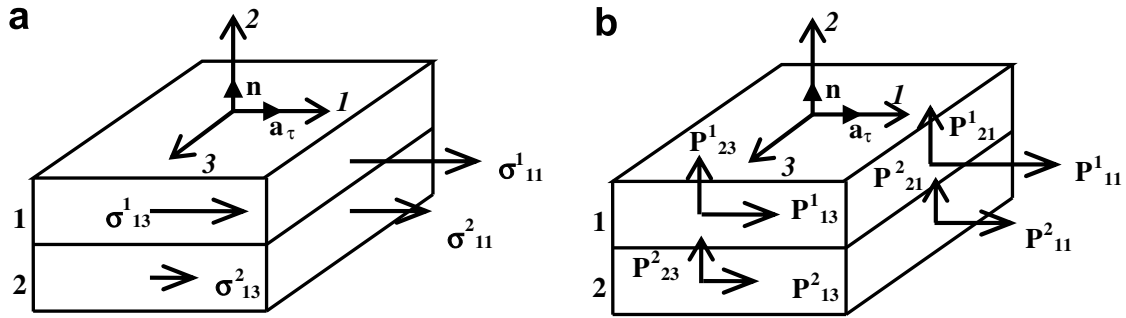
Fig. 2. Components of the stress tensor that are discontinuous across the interface $\Sigma$ and therefore contribute to the driving force for interface rotation $X_n$. (a) for small strains; (b) for finite strains in the reference configuration, where $P$ is the first nonsymmetric Piola–Kirchoff stress tensors (the force per unit area in the undeformed state).

Thus, the normal component of the strain discontinuity across the interface does not induce interface rotation; only the shear (volume preserving) component contributes to $X_n$. Also, $X_n \cdot n = 0$ because of $[\sigma] \cdot n = 0$, i.e., $X_n$ lies in the interface. In the coordinate system where $a_\tau = |a_\tau|(1,0,0)$ and $n = (0,1,0)$ (Fig. 2a) we have

$$X_n^1 = -c_1 c_2 |a_\tau| [\sigma_{11}] \quad \text{and} \quad X_n^3 = -c_1 c_2 |a_\tau| [\sigma_{13}], \tag{14}$$

i.e. the discontinuities in only two components of $\sigma$ contribute to $X_n$. Thus, the conditions for thermodynamic orientational equilibrium are

$$[\sigma_{11}] = [\sigma_{13}] = 0 \quad \text{or} \quad a_\tau = 0. \tag{15}$$

The same expressions for $X_n$ and $X_c$ hold for the volume $V$ that contains multiple evolving parallel plane interfaces between alternating phases 1 and 2. To further elaborate the effect of stresses on the interface reorientation, we assume for each phase the Hooke's law and additive decomposition of the total strain into elastic, $\varepsilon_i^e$, and transformation (eigen), $\varepsilon_i^t$, strains

$$\sigma_1 = E_1 : \varepsilon_1^e, \quad \sigma_2 = E_2 : \varepsilon_2^e, \tag{16}$$
$$\varepsilon_1 = \varepsilon_1^e + \varepsilon_1^t, \quad \varepsilon_2 = \varepsilon_2^e + \varepsilon_2^t, \tag{17}$$

where $E_i$ is the fourth-rank elasticity tensor. Transformation strains transform the crystal lattice of the parent phase into the lattice of the product phase; if phase 1 is considered as a parent phase, then $\varepsilon_1^t = 0$. Let the elastic properties of phases be the same, $E_1 = E_2 = E$, and $\varepsilon_2^t$ be independent of the applied stress $\sigma$. Then stresses in phases can be presented in the form $\sigma_i = \sigma + \sigma_i^{in}$, where $\sigma_i^{in}$ are the internal stresses, due to the transformation strain $\varepsilon_2^t$ (i.e. $c_1 \sigma_1^{in} + c_2 \sigma_2^{in} = 0$), that are independent of the external stresses $\sigma$. In this case, the jump in stress $[\sigma] = [\sigma^{in}]$ and consequently jump in strain $[\varepsilon] = [\varepsilon^e] + \varepsilon_2^t = [\sigma^{in}] : E^{-1} + \varepsilon_2^t$ and $a$ are independent of the external stresses $\sigma$. Thus, the driving force for reorientation $X_n$ is independent of the stresses $\sigma$ as well. If the interface is an invariant plane for $\varepsilon^t$ (see Wayman, 1964; Bhattacharya, 2004), for example, between two twins, then $\sigma^{in} = 0$ and again the external stresses will not cause interface rotation. Thus, for equal linear elastic properties of phases and stress-independent transformation strain, external stresses do not effect interface rotation. This is generally not true for equal nonlinear elastic properties (because the principle of linear superposition cannot be applied), for unequal linear or nonlinear elastic properties, and when $\varepsilon_2^t$ depends on external stresses $\sigma$ (e.g. when one phase consists of a fine-scale mixture of several crystallographically equivalent variants, see Section 4, or when plastic accommodation occurs). Since

$$\dot{c} = v_{0n}\Sigma/V, \tag{18}$$

where $v_{0n}$ is the velocity of translational motion of the parallel interfaces (the same for each interface) and $\Sigma$ is the total area of all interfaces, then Eq. (11) can be transformed to

$$D_V = X_\Sigma v_{0n} + \boldsymbol{X}_n \cdot \dot{\boldsymbol{n}} \geqslant 0, \tag{19}$$

where

$$X_\Sigma := X_c \Sigma/V \tag{20}$$

is the thermodynamic driving force conjugate to the translational interface velocity.

Let us transform the Eshelby driving force $X_c$ for linear elastic materials with

$$\psi_1 = \psi_1^e(\varepsilon_e) + \psi_1^\theta(\theta), \quad \psi_2 = \psi_2^e(\varepsilon_e) + \psi_2^\theta(\theta), \tag{21}$$
$$\psi_1^e(\varepsilon_e) = 0.5\boldsymbol{\varepsilon}_1^e : \boldsymbol{E}_1 : \boldsymbol{\varepsilon}_1^e, \quad \psi_2^e(\varepsilon_e) = 0.5\boldsymbol{\varepsilon}_2^e : \boldsymbol{E}_2 : \boldsymbol{\varepsilon}_2^e, \tag{22}$$

where $\psi^\theta$ and $\psi^e$ are the thermal and elastic parts of the free energy. First, multiplying $\boldsymbol{\sigma} = c_1\boldsymbol{\sigma}_1 + c_2\boldsymbol{\sigma}_2$ with $\boldsymbol{n}$ and using the traction continuity condition (9)$_2$, we obtain $\boldsymbol{n} \cdot \boldsymbol{\sigma} = c_1\boldsymbol{n} \cdot \boldsymbol{\sigma}_1 + c_2\boldsymbol{n} \cdot \boldsymbol{\sigma}_2 = \boldsymbol{n} \cdot \boldsymbol{\sigma}_1 = \boldsymbol{n} \cdot \boldsymbol{\sigma}_2$. Then employing the Hadamard compatibility condition (9)$_1$ and symmetry of the stress tensor, we derive $\boldsymbol{\sigma} : [\varepsilon] = \boldsymbol{n} \cdot \boldsymbol{\sigma} \cdot \boldsymbol{a} = \boldsymbol{n} \cdot \boldsymbol{\sigma}_1 \cdot \boldsymbol{a} = \boldsymbol{n} \cdot \boldsymbol{\sigma}_2 \cdot \boldsymbol{a} = \boldsymbol{\sigma}_1 : [\varepsilon] = \boldsymbol{\sigma}_2 : [\varepsilon] = 0.5(\boldsymbol{\sigma}_1 + \boldsymbol{\sigma}_2)[\varepsilon]$. Then

$$X_c = 0.5(\boldsymbol{\sigma}_1 + \boldsymbol{\sigma}_2) : [\boldsymbol{\varepsilon}^e + \boldsymbol{\varepsilon}^t] - [\psi^e + \psi^\theta] = 0.5(\boldsymbol{\sigma}_1 + \boldsymbol{\sigma}_2)$$
$$: (\boldsymbol{\varepsilon}_2^e - \boldsymbol{\varepsilon}_1^e) + 0.5(\boldsymbol{\sigma}_1 + \boldsymbol{\sigma}_2) : (\boldsymbol{\varepsilon}_2^t - \boldsymbol{\varepsilon}_1^t) - (\psi_2^e - \psi_1^e) + (\psi_2^\theta - \psi_1^\theta). \tag{23}$$

Using Hooke's law, we transform $0.5(\boldsymbol{\sigma}_1 + \boldsymbol{\sigma}_2) : (\boldsymbol{\varepsilon}_2^e - \boldsymbol{\varepsilon}_1^e) = 0.5(\boldsymbol{\varepsilon}_2^e : \boldsymbol{E}_2 : \boldsymbol{\varepsilon}_2^e - \boldsymbol{\varepsilon}_1^e : \boldsymbol{E}_1 : \boldsymbol{\varepsilon}_1^e - \boldsymbol{\varepsilon}_1^e : (\boldsymbol{E}_2 - \boldsymbol{E}_1) : \boldsymbol{\varepsilon}_2^e) = (\psi_2^e - \psi_1^e) - 0.5\boldsymbol{\varepsilon}_1^e : \Delta\boldsymbol{E} : \boldsymbol{\varepsilon}_2^e$. Inserting into Eq. (23), we finally obtain

$$X_c = 0.5(\boldsymbol{\sigma}_1 + \boldsymbol{\sigma}_2) : (\boldsymbol{\varepsilon}_2^t - \boldsymbol{\varepsilon}_1^t) - 0.5\boldsymbol{\varepsilon}_1^e : \Delta\boldsymbol{E} : \boldsymbol{\varepsilon}_2^e - (\psi_2^\theta - \psi_1^\theta). \tag{24}$$

## 3. Dissipation rate and kinetic equations

In this section we will derive several versions of the kinetic equations for the rate of volume fraction $\dot{c}$ (or translational interface velocity $v_{n0}$) and reorientation rate $\dot{\boldsymbol{n}}$ in terms of the thermodynamic driving forces $X_c$ (or $X_\Sigma$) and $\boldsymbol{X}_n$. Based on physical mechanisms of the resistance to an interface motion (interface friction) and their modeling, we will take into account two types of the interface friction (Grujicic and Olson, 1985; Grujicic et al., 1985; Olson and Cohen, 1986):

(i) Athermal friction due to interaction between the interface and the long-range stress fields of defects (point defects, dislocations, grain and subgrain boundaries), as well as the Peierls barrier and acoustic emission. It is similar to the dry friction for rigid body motion along the plane and causes threshold-type resistance.

(ii) Viscous linear friction due to phonon drag mechanisms. Since local interface velocity during martensitic plate growth can be of the order of magnitude of km/s, this term plays an important role (Olson and Cohen, 1986). However, since martensitic plate is getting arrested fast, e.g. by grain boundary or other plates, in macroscopic modeling this event is considered as instantaneous and viscous term is neglected. In local description as well as for high-strain loading, it has to be taken into account.

Other contributions, for example, dissipation due to thermally activated motion of the interface passing obstacles (Grujicic and Olson, 1985; Grujicic et al., 1985; Olson and Cohen, 1986), can be similarly taken into account.

### 3.1. Linear kinetic relationships

The simplest linear relationships between the thermodynamic forces and rates can be obtained assuming quadratic expression for the dissipation rate in terms of thermodynamic forces

$$D_{X_c}(X_c, \boldsymbol{X}_n) = h_c X_c^2 + 2\boldsymbol{m}_c \cdot \boldsymbol{X}_n X_c + \boldsymbol{X}_n : \boldsymbol{h}_n : \boldsymbol{X}_n \geqslant 0 \tag{25}$$

with $h_c$, $\boldsymbol{m}_c$ and $\boldsymbol{h}$ as scalar, vector and symmetric second-rank tensor parameters. We keep the most general anisotropic form since a priori the problem contains various vector and tensor parameters (like $\boldsymbol{\sigma} \cdot \boldsymbol{n}$, $\boldsymbol{a}$ and $\boldsymbol{\varepsilon}_t$) that can generate the vector $\boldsymbol{m}_c$ and tensor $\boldsymbol{h}_n$. Using extremum principle of linear thermodynamics (Haase, 1969; Ziegler, 1977), we obtain the relationships

$$\dot{c} = \frac{1}{2}\frac{\partial D_{X_c}}{\partial X_c} = h_c X_c + \boldsymbol{m}_c \cdot \boldsymbol{X}_n, \quad \dot{\boldsymbol{n}} = \frac{1}{2}\frac{\partial D_{X_c}}{\partial \boldsymbol{X}_n} = \boldsymbol{m}_c X_c + \boldsymbol{h}_n : \boldsymbol{X}_n \tag{26}$$

that incorporate the Onsager reciprocity relationships. Usually, $\boldsymbol{m} = 0$. These relationships can be easily inverted. Alternatively, we can start with

$$D_{X_\Sigma}(X_\Sigma, \boldsymbol{X}_n) = h_\Sigma X_\Sigma^2 + 2\boldsymbol{m}_\Sigma \cdot \boldsymbol{X}_n X_\Sigma + \boldsymbol{X}_n : \boldsymbol{h}_n : \boldsymbol{X}_n \geqslant 0 \tag{27}$$

and obtain

$$v_{n0} = \frac{1}{2}\frac{\partial D_{X_\Sigma}}{\partial X_\Sigma} = h_\Sigma X_\Sigma + \boldsymbol{m}_\Sigma \cdot \boldsymbol{X}_n,$$
$$\dot{\boldsymbol{n}} = \frac{1}{2}\frac{\partial D_{X_\Sigma}}{\partial \boldsymbol{X}_n} = \boldsymbol{m}_\Sigma X_\Sigma + \boldsymbol{h}_n : \boldsymbol{X}_n. \tag{28}$$

Substituting Eqs. (18) and (20) into Eq. (26) or (28) one derives

$$h_c = h_\Sigma \left(\frac{\Sigma}{V}\right)^2, \quad \boldsymbol{m}_c = \boldsymbol{m}_\Sigma \frac{\Sigma}{V}. \tag{29}$$

If one considers single interface propagating through the parallelepiped, the area $\Sigma$ varies from zero to maximum value and then again to zero. Thus, choosing $h_\Sigma$ and $\boldsymbol{m}_\Sigma$ constant, one obtains variable $h_c$ and $\boldsymbol{m}_c$ and vice versa. Consequently, the choice of $D_{X_\Sigma}$ or $D_{X_c}$ as a primary function is a constitutive assumption that has to be justified. Below we will perform this in detail. If there is a large amount of interfaces (like in martensitic $M_I$–$M_{II}$ mixture), then the total interface area is almost constant during the chance in volume fraction and both choices are approximately equivalent (Figs. 1c and d).

### 3.2. Dissipation rate for three-dimensional geometry

Here we will calculate the dissipation rate due to the phase transformation and interface reorientation by explicitly considering the single or multiple parallel interface motion. The dissipation rate at each point of the moving interface is assumed to be the sum of athermal, $\mathscr{D}_a$, and viscous, $\mathscr{D}_v$, friction components:

$$\mathscr{D} = \mathscr{D}_a + \mathscr{D}_v = k|v_n| + \lambda v_n^2. \tag{30}$$

Here $v_n$ is the normal interface velocity, $k$ is the athermal interface friction and $\lambda$ is the viscosity coefficient. The dissipation rate per unit volume due to the motion of the interface is

$$D = \int_\Sigma \mathscr{D}\, d\Sigma / V = D_a + D_v. \tag{31}$$

For a plane interface, the normal velocity at the point $\boldsymbol{r}$ can be expressed as

$$v_n = v_{0n} + \boldsymbol{n} \cdot \boldsymbol{\omega} \times (\boldsymbol{r} - \boldsymbol{r}_0), \tag{32}$$

where $\boldsymbol{r}_0$ is the centroid of the interface in $V$, $v_{0n} = \dot{\boldsymbol{r}}_0 \cdot \boldsymbol{n}$ is the normal velocity of the centroid, and $\boldsymbol{\omega} = \boldsymbol{n} \times \dot{\boldsymbol{n}}$ ($|\boldsymbol{\omega}| = |\dot{\boldsymbol{n}}|$) is the angular velocity of the interface. Then one obtains for the viscous dissipation

$$VD_v = \lambda \int_\Sigma (v_{0n} + \boldsymbol{n} \cdot \boldsymbol{\omega} \times (\boldsymbol{r} - \boldsymbol{r}_0))^2\, d\Sigma = \lambda(v_{0n}^2 \Sigma - \boldsymbol{n} \cdot \boldsymbol{\omega} \times \boldsymbol{J} \times \boldsymbol{\omega} \cdot \boldsymbol{n}), \tag{33}$$

where $\int_\Sigma (\boldsymbol{r} - \boldsymbol{r}_0)\, d\Sigma = 0$ is taken into account (by definition of the centroid) and $\boldsymbol{J} := \int_\Sigma (\boldsymbol{r} - \boldsymbol{r}_0)(\boldsymbol{r} - \boldsymbol{r}_0)\, d\Sigma$ is the tensor of the centroidal moment of inertia of the interface. Note that despite the sign "$-$" in Eq. (33), the second term related to $\boldsymbol{\omega}$ is of course positive. If multiple parallel interfaces move with the same translational and angular velocity, then in Eq. (33) $\Sigma$ is their total area and $\boldsymbol{J}$ is the sum of the centroidal moments of inertia for all interfaces. One of the main results is that *there is no coupling term between translational and angular velocity*, i.e. $\boldsymbol{m}_c = \boldsymbol{m}_\Sigma = 0$ in (26) and (28) and in particular, $X_\Sigma = \lambda \frac{\Sigma}{\Sigma} v_{0n}$ and $X_c = \lambda v_{0n}$. To find relationship $X_n(\dot{\boldsymbol{n}})$, we represent $-\boldsymbol{n} \cdot \boldsymbol{\omega} \times \boldsymbol{J} \times \boldsymbol{\omega} \cdot \boldsymbol{n} = K_{lq}\dot{n}_l\dot{n}_q$ in the component form with $K_{lq} := \epsilon^{ikj}\epsilon^{amc}\epsilon^{jdl}\epsilon^{cpq}J_{km}n_i n_p n_d n_a$ and $\epsilon^{ikl}$ for components of Levi–Civita permutating tensor in orthonormal basis $\boldsymbol{e}_i$. Then, $X_n^l = \lambda K_{lq}\dot{n}_q / V$.

For the athermal dissipation we derive

$$\begin{aligned}
VD_a &= k \int_\Sigma |v_{0n} + \boldsymbol{n} \cdot \boldsymbol{\omega} \times (\boldsymbol{r} - \boldsymbol{r}_0)|\, d\Sigma \\
&= k\left( \int_{\Sigma_+} (v_{0n} + \boldsymbol{n} \cdot \boldsymbol{\omega} \times (\boldsymbol{r} - \boldsymbol{r}_0))\, d\Sigma - \int_{\Sigma_-} (v_{0n} + \boldsymbol{n} \cdot \boldsymbol{\omega} \times (\boldsymbol{r} - \boldsymbol{r}_0))\, d\Sigma \right) \\
&= k v_{0n}(\Sigma_+ - \Sigma_-) + k\boldsymbol{n} \cdot \boldsymbol{\omega} \times \left( \int_{\Sigma_+} (\boldsymbol{r} - \boldsymbol{r}_0)\, d\Sigma \right) - \left( \int_{\Sigma_-} (\boldsymbol{r} - \boldsymbol{r}_0)\, d\Sigma \right),
\end{aligned} \tag{34}$$

where $\Sigma_+$ and $\Sigma_-$ are parts of the interface $\Sigma$ where $v_n > 0$ and $v_n < 0$, respectively. Since these parts depend both on $v_{0n}$ and $\boldsymbol{\omega}$, explicit expression for $D_a$ in terms of $v_{0n}$ and $\boldsymbol{\omega}$ is bulky in general case. Only in the case when the normal interface velocity does not change the sign within the interface, one obtains

$$D_a = k|v_{0n}|\Sigma/V = k|\dot{c}| \tag{35}$$

and the term with $\boldsymbol{\omega}$ disappears by definition of the centroid. For this case (as well as for $\boldsymbol{\omega} = 0$), expressions for the dissipation rate per unit volume

$$X_c \dot{c} = X_\Sigma v_{0n} = (k|v_{0n}| + \lambda v_{0n}^2)\Sigma/V = k|\dot{c}| + \lambda \dot{c}^2 V/\Sigma \tag{36}$$

result in

$$X_c = k\text{sign}(\dot{c}) + \lambda\dot{c}V/\Sigma = k\text{sign}(v_{0n}) + \lambda v_{0n},$$
$$X_\Sigma = (k\text{sign}(v_{0n}) + \lambda v_{0n})\Sigma/V. \tag{37}$$

Eq. (37) can be resolved for the rates:

$$v_{0n} = \frac{1}{\lambda}(X_c - k\text{sign}(X_c))H(|X_c| - k)$$
$$= \frac{1}{\lambda}\left(X_\Sigma\frac{V}{\Sigma} - \text{sign}\left(X_\Sigma\frac{V}{\Sigma}\right)\right)H\left(\left|X_\Sigma\frac{V}{\Sigma}\right| - k\right),$$
$$\dot{c} = \frac{\Sigma}{\lambda V}(X_c - k\text{sign}(X_c))H(|X_c| - k), \tag{38}$$

where $\text{sign}(\ldots)$ is the sign function and $H(a)$ is the Heaviside unit step function (i.e. $H(a) = 1$ for $a \geqslant 0$ and $H(a) = 0$ for $a < 0$). In more detail Eq. (38) can be presented in the form

$$\dot{c} = \frac{\Sigma}{\lambda V}(X_c - k) \quad \text{for } X_c > k,$$
$$\dot{c}, = \frac{\Sigma}{\lambda V}(X_c + k) \quad \text{for } X_c < -k, \tag{39}$$
$$\dot{c} = 0 \quad \text{for } |X_c| < k.$$

Similar expression is valid for $v_{0n}$. Important conclusion follows from Eqs. (37) to (38): while relationship $v_{0n}(X_c)$ is scale independent, the effective viscosity $\lambda V/\Sigma$ in relationship $\dot{c}(X_c)$ grows proportionally to the size of the volume $V$ for geometrically similar interface configurations. The condition for thermodynamic equilibrium, $|X_c| < k$, is scale independent. Both these results also follow from the dimension analysis.

To obtain all results analytically, we consider interface rotation in the plane 1–2. In this case, $v_n = v_{0n} + \omega r$, where $r$ is the distance from the interface centroid in the plane 1–2, $[\sigma_{13}] = 0$, $\boldsymbol{X}_n = X_n\boldsymbol{a}_\tau/|\boldsymbol{a}_\tau|$, and $\boldsymbol{X}_n \cdot \boldsymbol{n} = X_n\omega$.

### 3.3. Single interface

We have for the dissipation rate

$$VD = \int_\Sigma k|v_n|d\Sigma + \int_\Sigma \lambda v_n^2 d\Sigma = kb\int_{-R}^R |v_n|dr + \lambda b\int_{-R}^R v_n^2 dr, \tag{40}$$

where $d\Sigma = b\,dr$ and $b = 1$ is the depth of the parallelepiped. The viscous dissipation, $D_v$, is equal to

$$SD_v = \lambda\int_{-R}^R v_n^2 dr = \lambda\omega^2\int_{-R}^R (r - r_c)^2 dr = \frac{2\lambda\omega^2 R(R^2 + 3r_c^2)}{3}, \tag{41}$$

where $S$ is the area of the parallelepiped face. When evaluating $D_a$, one needs to consider separately the cases when the position of the center of rotation $r_c = -v_{0n}/\omega$ belongs to the interface ($-R \leqslant r_c \leqslant R$, where $2R$ is the interface length in the plane 1–2), or does not, i.e. when $v_n$ is of fixed sign or changes sign within the interface.

**Case 1.** $-R < r_c < R$ (which, after substitution $r_c = -v_{0n}/\omega$ and introducing the 'angular' velocity $\omega_0 := v_0/R$ related to translational velocity $v_0$, corresponds to $-1 < \omega_0/\omega < 1$). In this case

$$SD_a = k \int_{-R}^{R} |v_n| \mathrm{d}r = k|\omega| \int_{-R}^{R} |r - r_c| \mathrm{d}r$$

$$= k|\omega| \left( -\int_{-R}^{r_c} (r - r_c)\mathrm{d}r + \int_{r_c}^{R} (r - r_c)\mathrm{d}r \right) = k|\omega|(r_c^2 + R^2). \tag{42}$$

**Case 2.** $r_c < -R$ ($\omega_0/\omega > 1$). Simple calculations results in

$$SD_a = k|\omega| \int_{-R}^{R} (r - r_c)\mathrm{d}r = -2k|\omega|Rr_c = \frac{2k|\omega|Rv_0}{\omega} = \frac{2k|\omega|R^2\omega_0}{\omega}. \tag{43}$$

**Case 3.** $r_c > R$ ($\omega_0/\omega < -1$). In a similar way one obtains

$$SD_a = k|\omega| \int_{-R}^{R} (r_c - r)\mathrm{d}r = 2k|\omega|Rr_c = \frac{-2k|\omega|Rv_0}{\omega} = \frac{-2k|\omega|R^2\omega_0}{\omega}. \tag{44}$$

Combining all three cases together, we obtain after simple algebra

$$\begin{aligned}
D_a &= A|\omega|\left(1 + \frac{\omega_0^2}{\omega^2}\right) \text{ for } |\omega_0/\omega| \leqslant 1, \\
D_a &= 2A|\omega_0| \quad \text{for } \left|\frac{\omega_0}{\omega}\right| > 1, \\
D_v &= B\omega^2\left(1 + 3\frac{\omega_0^2}{\omega^2}\right), D = D_a + D_v,
\end{aligned} \tag{45}$$

where $A = kR^2/S$ and $B = 2\lambda R^3/(3S)$. It is clear that for corresponding to each other generalized forces and rates, $D_V = D$. Normalizing the dissipation rate by $A$ and choosing $\omega_0$ and $\omega$ as generalized rates we obtain from Eq. (19)

$$\widetilde{D}_V := \frac{D_V}{A} = \widetilde{X}_c\omega_0 + \widetilde{X}_n\omega, \quad \widetilde{X}_c = \frac{X_cR\Sigma}{AV} \quad \text{and} \quad \widetilde{X}_n = \frac{X_n}{A}. \tag{46}$$

Similarly, normalizing the dissipation function Eq. (45) $\widetilde{D}(\omega_0, \omega) := D/A$, one obtains for corresponding to each other generalized forces and rates

$$\widetilde{D}_V = \widetilde{X}_c\omega_0 + \widetilde{X}_n\omega = \widetilde{D}(\omega_0, \omega). \tag{47}$$

Single Eq. (47) cannot determine two scalar driving forces $\widetilde{X}_c, \widetilde{X}_n$. Usually, the extremum principles of nonlinear irreversible thermodynamics formulated in Ziegler (1977) can be used. These principles have been justified using the postulate of realizability (Levitas, 1995). However, direct application of such principles to Eq. (47) leads to contradictory results, which couples in a complex and unnatural way athermal and viscous parts of dissipative forces. To resolve the contradiction, we decompose the dissipation function and the driving forces $\widetilde{X}$ into athermal and viscous parts, i.e. $\widetilde{D} = \widetilde{D}_a + \widetilde{D}_v$, $\widetilde{X}_c = \widetilde{X}_c^a + \widetilde{X}_c^v$ and $\widetilde{X}_n = \widetilde{X}_n^a + \widetilde{X}_n^v$. Then we obtain

$$\begin{aligned}
\widetilde{D}_a &:= D_a/A = \widetilde{X}_c^a\omega_0 + \widetilde{X}_n^a\omega = \widetilde{\boldsymbol{X}}^a \cdot \bar{\boldsymbol{\omega}}, \\
\widetilde{D}_v &:= D_v/A = \widetilde{X}_c^v\omega_0 + \widetilde{X}_n^v\omega = \widetilde{\boldsymbol{X}}^v \cdot \bar{\boldsymbol{\omega}},
\end{aligned} \tag{48}$$

where $D_a$ and $D_v$ are given by Eq. (45), and we introduced two-dimensional vectors of generalized rates $\bar{\omega} := (\omega, \omega_0)$, as well as athermal $\widetilde{X}^a := (\widetilde{X}_n^a, \widetilde{X}_c^a)$ and viscous thermodynamic forces $\widetilde{X}^v := (\widetilde{X}_n^v, \widetilde{X}_c^v)$ thermodynamic forces; $\widetilde{X} := \widetilde{X}^a + \widetilde{X}^v$. Two Eqs. (48) are again not sufficient to find the four scalar driving forces $\widetilde{X}^a$, $\widetilde{X}^v$. However, now we can apply the extremum principles of nonlinear irreversible thermodynamics (Ziegler, 1977; Levitas, 1995) to athermal and viscous driving force separately. The general relationship between the conjugate dissipative force, $X$, and rate, $\dot{q}$ (i.e. the dissipation rate is $D := X \cdot \dot{q}$), is

$$X = z\frac{\mathrm{d}D}{\mathrm{d}\dot{q}}, \quad z = D\left(\frac{\mathrm{d}D}{\mathrm{d}\dot{q}} \cdot \dot{q}\right)^{-1}. \tag{49}$$

If the dissipation function $D(\dot{q})$ is a homogeneous function of degree $n$, i.e. $D(l\dot{q}) = l^n D(\dot{q})$, then according to Euler's theorem for homogeneous functions, $\frac{\mathrm{d}D}{\mathrm{d}\dot{q}} \cdot \dot{q} = nD$ and $z = 1/n$. The athermal dissipation is a homogeneous function of degree 1 (i.e. $z = 1$) and viscous dissipation is a homogeneous function of degree 2 (i.e. $z = 1/2$). Thus, we obtain

$$\widetilde{X}_c^a = \frac{\partial \widetilde{D}_a}{\partial \omega_0} = \begin{cases} \frac{2\omega_0}{\omega}\mathrm{sign}(\omega) & \text{for } \left|\frac{\omega_0}{\omega}\right| \leqslant 1 \\ 2\mathrm{sign}(\omega_0) & \text{for } \left|\frac{\omega_0}{\omega}\right| > 1 \end{cases},$$

$$\widetilde{X}_n^a = \frac{\partial \widetilde{D}_a}{\partial \omega} = \begin{cases} \left(1 - \frac{\omega_0^2}{\omega^2}\right)\mathrm{sign}(\omega) & \text{for } \left|\frac{\omega_0}{\omega}\right| \leqslant 1 \\ 0 & \text{for } \left|\frac{\omega_0}{\omega}\right| > 1 \end{cases}, \tag{50}$$

$$\widetilde{X}_c^v = 0.5\frac{\partial \widetilde{D}_v}{\partial \omega_0} = 3C\omega_0, \quad \widetilde{X}_n^v = 0.5\frac{\partial \widetilde{D}_v}{\partial \omega} = C\omega, \quad C := \frac{B}{A}. \tag{51}$$

Let us consider the case $\widetilde{X}^v \ll \widetilde{X}^a$, which corresponds to neglect of viscosity ($C = 0$) or slow interface motion, i.e. interface rotation and propagation. Eliminating $\omega_0/\omega$ from Eq. (50) for $|\omega_0/\omega| \leqslant 1$, one obtains the equations of the limit curve for interface motion in the $\widetilde{X}_n^a - \widetilde{X}_c^a$ plane (Fig. 3)

$$f_{\pm}(\widetilde{X}^a) := \pm\widetilde{X}_n^a - [1 - 0.25(\widetilde{X}_c^a)^2] = 0, \tag{52}$$

where $f_+$ ($f_-$) corresponds to $\mathrm{sign}(\omega) = +1$ ($\mathrm{sign}(\omega) = -1$). The case $|\omega_0/\omega| > 1$ yields just two points $\widetilde{X}^a = (0, \pm 2)$ that in any case belong to the curve (52). Inside the curve (52), i.e. for $f < 0$, where $\omega_0 = \omega = 0$, the interface motion does not occur. The curve $f = 0$ is the counterpart of the yield surface for single and polycrystalline plasticity in stress space (Lubliner, 1990) or the friction surface (Levitas, 1995), or the phase transformation surface in stress space (Levitas, 1992; Sun and Hwang, 1993; Levitas et al., 1999). In fact, the dissipation function and all relationships that we found will be the same for a rigid line sliding with rotation along the plane surface and subjected to dry and viscous friction. It is known for these systems that the potential-type relationships (50) result in the potential-type inverse relationships

$$\bar{\omega} = h\frac{\mathrm{d}f}{\mathrm{d}\widetilde{X}^a} \tag{53}$$

with a constant $h > 0$. Thus, the vector $\bar{\omega}$ is a normal to the limit curve $f = 0$ (Fig. 3). This is so-called associated phase transformation rule (normality rule) similar to the normality rule for phase transformation (Levitas, 1992; Sun and Hwang, 1993; Levitas et al., 1999)
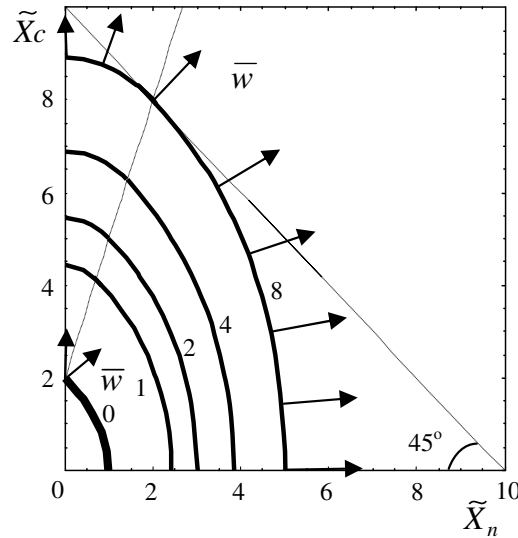
Fig. 3. Plots of the potential contours $\Psi(\widetilde{X}) = M$ for the values of $M$ shown near the curves. The contours are symmetric with respect to the $\widetilde{X}_n$ and $\widetilde{X}_c$ axes. The contour $\Psi = 0$ coincides with $f = 0$ (Eq. (52)), inside of which interface motion does not occur. The velocity vector $\bar{\omega}$ is orthogonal to the potential contours; its magnitude is proportional to the inverse distance between the nearest curves along $\bar{\omega}$. The straight line $\widetilde{X}_c - 3\widetilde{X}_n = 2$ corresponds to the condition $\omega_0 = \omega$. The curves above the line $\widetilde{X}_c - 3\widetilde{X}_n = 2$ are ellipses.

and plasticity (Lubliner, 1990), in stress space and for system with friction (Levitas, 1995). In more detail,

$$\omega_0 = h\frac{\partial f}{\partial \widetilde{X}_c^a} = 0.5h\widetilde{X}_c^a, \quad \omega = h\frac{\partial f}{\partial \widetilde{X}_n^a} = \pm h, \quad \frac{\omega_0}{\omega} = \pm 0.5\widetilde{X}_c^a = \pm(1 \pm \widetilde{X}_n^a)^{0.5}, \qquad (54)$$

where Eq. (52) has been used to express $\widetilde{X}_c^a$ in terms of $\widetilde{X}_n^a$. At the singular points $\widetilde{X}^a = (\pm 2, 0)$, where the normal is ambiguous, the vector $\bar{\omega}$ is a linear combination of the normals to the surfaces $f_+$ and $f_-$:

$$
\begin{aligned}
\omega_0 &= h_1\frac{\partial f_+}{\partial \widetilde{X}_c^a} + h_2\frac{\partial f_-}{\partial \widetilde{X}_c^a} = 0.5(h_1 + h_2)\widetilde{X}_c^a, \\
\omega &= h_1\frac{\partial f_+}{\partial \widetilde{X}_n^a} + h_2\frac{\partial f_-}{\partial \widetilde{X}_n^a} = (h_1 - h_2), \\
\frac{\omega_0}{\omega} &= 0.5\frac{h_1 + h_2}{h_1 - h_2}\widetilde{X}_c^a = \frac{h_1 + h_2}{h_1 - h_2}(1 \pm \widetilde{X}_n^a)^{0.5},
\end{aligned}
\qquad (55)
$$

where $h_1 > 0$ and $h_2 > 0$ are constants. Since $\frac{h_1+h_2}{h_1-h_2}$ varies in the intervals $(-\infty; -1]$ and $[1; \infty]$, the vector $\bar{\omega}$ lies on or between the normals to the surfaces $f_+$ and $f_-$, which are inclined $\pm 45°$ to the $\widetilde{X}_c^a$ axis (Fig. 3). Since $\omega$ must vanish for $\widetilde{X}_n^a = 0$ (i.e. for zero driving force for rotation and due to symmetry), $\bar{\omega}$ is along the $\widetilde{X}_c^a$ axis. However, for any positive infinitesimal $\widetilde{X}_n^a$ we get $\omega_0/\omega = 1$, for any negative infinitesimal $\widetilde{X}_n^a$ we obtain $\omega_0/\omega = -1$, i.e. $\omega$ jumps by a finite value. This means that during the interface propagation, the interface rotation occurs fast until the thermodynamic equilibrium orientation determined by $\widetilde{X}_n^a = 0$ is reached. In contrast, since there is no singular point on the curve $f = 0$ for $\widetilde{X}_c^a = 0$, an infinitesimal $\widetilde{X}_c^a$ causes an infinitesimal interface propagation; for $\widetilde{X}_c^a = 0$, only interface rotation occurs. Also, for any $\widetilde{X}_n^a \neq 0$, the center of interface rotation belongs to the interface and $|\omega_0/\omega| \leqslant 1$.

In the case $\overline{X}^{a} \ll \overline{X}^{v}$, i.e., small athermal friction or large viscosity, Eq. (51) shows that there is no coupling between interface propagation and interface rotation.

Consider now a system in thermodynamic equilibrium with $\widetilde{X}_{n}^{a} \neq 0$ and $f < 0$, and increase $|\widetilde{X}_{c}^{a}|$ by changing the temperature until $f = 0$. Then, interface rotation will occur along with interface propagation until $\widetilde{X}_{n}^{a} = 0$. Since $|\widetilde{X}_{c}^{a}| = 2\sqrt{1 - |\widetilde{X}_{n}^{a}|}$, a rotational driving force ($\widetilde{X}_{n}^{a} \neq 0$) can significantly reduce the magnitude of the driving force required for interface propagation.

It is more convenient in calculations to use kinetic equations, i.e. relationships of the generalized rates on the thermodynamic forces $\bar{\omega}(\widetilde{X})$. With viscous friction, Eqs. (50) and (51) are of the potential form $\widetilde{X}(\bar{\omega}) = \mathrm{d}\Phi/\mathrm{d}\bar{\omega}$, where the dissipative potential $\Phi = \widetilde{D}_{a} + \widetilde{D}_{v}/2$. Using the Legendre transformation $\Psi(\widetilde{X}) = \widetilde{X} \cdot \bar{\omega}(\widetilde{X}) - \Phi(\bar{\omega}(\widetilde{X}))$, one can invert the relations between $\bar{\omega}$ and $\widetilde{X}$:

$$\bar{\omega} = \frac{\mathrm{d}\Psi}{\mathrm{d}\widetilde{X}}, \tag{56}$$

where

$$\Psi(\widetilde{X}) = g_{3}\left[ 2^{2/3}g_{4}\left(\widetilde{X}_{n} - \left(1 + \frac{1}{182^{1/3}g_{4}^{2}}\right)\right) - 2^{1/3}g_{3}g_{4}^{2}\left(1 + \frac{1}{62^{1/3}g_{4}^{2}}\right) + \frac{\widetilde{X}_{c}}{3}\right]\frac{1}{C}$$

$$\text{for } \widetilde{X}_{c} - 3\widetilde{X}_{n} \leqslant 2,$$

$$\Psi(\widetilde{X}) = \frac{(\widetilde{X}_{c} - 2)^{2} + 3\widetilde{X}_{n}^{2}}{6C} \text{ for } \widetilde{X}_{c} - 3\widetilde{X}_{n} > 2. \tag{57}$$

Here $g_{1} = (9\widetilde{X}_{c} + (81\widetilde{X}_{c}^{2} + 4(3\widetilde{X}_{n} - 1)^{3})^{1/2})^{1/3}$, $g_{2} = 2 - 6\widetilde{X}_{n} + 2^{1/3}g_{1}^{2}$, $g_{3} = \widetilde{X}_{c} - 2^{1/3}/(3g_{4})$, and $g_{4} = g_{1}/g_{2}$. For $\widetilde{X}_{c}, \widetilde{X}_{n} > 0$, $\bar{\omega}(\widetilde{X})$ is given by

$$\omega_{0} = \frac{g_{3}}{3C}, \quad \omega = 2^{2/3}g_{3}\frac{g_{4}}{C} \text{ for } \widetilde{X}_{c} - 3\widetilde{X}_{n} \leqslant 2, \quad \omega_{0} = \frac{\widetilde{X}_{c} - 2}{3C},$$

$$\omega = \frac{\widetilde{X}_{n}}{C} \text{ for } \widetilde{X}_{c} - 3\widetilde{X}_{n} > 2. \tag{58}$$

A geometric representation of Eqs. (57) and (58) is given in Fig. 3: vector $\bar{\omega}$ is orthogonal to the level curves of the potential $\Psi(\widetilde{X})$ in the plane of the thermodynamic forces $\widetilde{X}$. Viscosity regularizes the singular point on the limit curve $f = 0$ (or $\Psi = 0$) and removes the jump in the $\bar{\omega}$ vector. Outside the limit curve $f = 0$, an infinitesimal $\widetilde{X}_{n}$ causes an infinitesimal interface rotation rate. Eq. (58) is simple because it corresponds to the singular point of the curve $f = 0$, i.e. $\widetilde{X}^{a} = (0, 2)$. That is why $\omega$ is described by pure viscous rule and $\omega_{0}$ is described by viscous rule under the action of "overforce" (i.e. difference between $\widetilde{X}_{c}$ and the athermal threshold for interface propagation equal to 2).

### 3.4. Multiple interfaces

The initial calculations of the dissipation function for multiple parallel interfaces is similar to the case of a single interface but with summation of integrals over all interfaces in Eqs. (40)–(44). Since $v_{0n}$ and $\omega$ are assumed to be the same for each interface, the position of the center of rotation $r_{c} = -v_{0n}/\omega$ is also the same for each interface. Then the viscous dissipation, $D_{v}$, is equal to

$$SD_{v} = \lambda \sum_{i=1}^{n} \int_{-R_{i}}^{R_{i}} v_{n}^{2}\,\mathrm{d}r = 2\lambda\omega^{2}\left(\sum_{i=1}^{n} R_{i}^{3} + 3r_{c}^{2}\sum_{i=1}^{n} R_{i}\right)\Big/3. \tag{59}$$

Introducing characteristic size, $\overline{R}$, and angular velocity, $\omega_0$ by equations

$$\overline{R} := \sqrt{\sum_{i=1}^{n} R_i^3 \Big| \Big/ \sum_{i=1}^{n} R_i}, \quad \omega_0 := \frac{v_0}{\overline{R}}, \tag{60}$$

we obtain

$$D_v = \overline{B}\omega^2 \left(1 + 3\frac{\omega_0^2}{\omega^2}\right), \quad \overline{B} := \frac{2\lambda\sum_{i=1}^{n} R_i^3}{3S}, \tag{61}$$

which has the same structure as Eq. $(45)_2$ and reduces to it when $n = 1$. If all $R_i$ are the same, then $\overline{B} = nB$. For the athermal dissipation we have to distinguish several cases.

**Case 1.** When the center of rotation is outside of any interface, i.e. $|r_c| > R_i^{\max}$ or $|\frac{\omega_0}{\omega}| > \widetilde{R}_i$, where $\widetilde{R}_i := \frac{R_i^{\max}}{\overline{R}}$, then

$$SD_a = k \left| \omega \sum_{i=1}^{n} \int_{-R_i}^{R_i} (r - r_c)\mathrm{d}r \right| = 2k|\omega||r_c| \sum_{i=1}^{n} R_i \tag{62}$$

and

$$D_a = 2\overline{A}|\omega_0|, \quad \overline{A} := k\overline{R} \sum_{i=1}^{n} R_i/S = P \sum_{i=1}^{n} \widetilde{R}_i, \quad P := \frac{k\overline{R}^2}{S}. \tag{63}$$

Eq. (63) has the same structure as Eq. $(45)_1$ and reduces to it when $n = 1$. If all $R_i$ are the same, then $\overline{A} = nA$.

**Case 2.** When the center of rotation belongs to each interface, i.e. $|r_c| \leqslant R_i$ or $|\frac{\omega_0}{\omega}| \leqslant \widetilde{R}$ for all $i$, then

$$SD_a = k|\omega| \sum_{i=1}^{n} \int_{-R_i}^{R_i} |r - r_c|\mathrm{d}r = k|\omega| \left(nr_c^2 + \sum_{i=1}^{n} R_i^2\right) \tag{64}$$

and

$$D_a = P|\omega|\left(Q + n\frac{\omega_0^2}{\omega^2}\right), \quad Q := \sum_{i=1}^{n} \widetilde{R}_i^2. \tag{65}$$

The structure of Eq. (65) is slightly different from the structure of Eq. $(45)_1$, since $Q \neq 1$; however, it reduces to it when $n = 1$. If all $R_i$ are the same, then $Q = n$ and $P = A$. The case when the center of rotation belongs to some interfaces and does not belong to others will be considered below. Dissipative forces are defined from the expression for the dissipation rate

$$D_V := \overline{X}_c\omega_0 + \overline{X}_n\omega = \overline{\boldsymbol{X}} \cdot \bar{\boldsymbol{\omega}}, \quad \overline{X}_c := \frac{X_c\overline{R}\Sigma}{V} \quad \text{and} \quad \overline{X}_n = X_n. \tag{66}$$

We defined $\overline{\boldsymbol{X}} := (\overline{X}_n, X_c)$ and $\overline{\boldsymbol{X}} = \overline{\boldsymbol{X}}^a + \overline{\boldsymbol{X}}^n$. For the above expressions for $D_a$ and $D_v$, we can obtain all equations similar to the case with the single interface. Thus,

$$\overline{X}^{\mathrm{a}}_c = \frac{\partial D_{\mathrm{a}}}{\partial \omega_0} = \begin{cases} 2Pn\frac{\omega_0}{\omega}\,\mathrm{sign}(\omega) & \text{for } \left|\frac{\omega_0}{\omega}\right| \leqslant \widetilde{R}_i \forall i \\ 2\overline{A}\,\mathrm{sign}(\omega_0) & \text{for } \left|\frac{\omega_0}{\omega}\right| > \widetilde{R}^{\mathrm{max}}_i \end{cases},$$

$$X^{\mathrm{a}}_n = \frac{\partial D_{\mathrm{a}}}{\partial \omega} = \begin{cases} P\left(Q - n\frac{\omega_0^2}{\omega^2}\right)\mathrm{sign}(\omega) & \text{for } \left|\frac{\omega_0}{\omega}\right| \leqslant \widetilde{R}_i \forall i \\ 0 & \text{for } \left|\frac{\omega_0}{\omega}\right| > \widetilde{R}^{\mathrm{max}}_i \end{cases}, \tag{67}$$

$$\overline{X}^{\mathrm{v}}_c = 0.5\frac{\partial D_{\mathrm{v}}}{\partial \omega_0} = 3\overline{B}\omega_0, \quad X^{\mathrm{v}}_n = 0.5\frac{\partial D_{\mathrm{v}}}{\partial \omega} = \overline{B}\omega. \tag{68}$$

For neglected viscosity ($C = 0$), eliminating $\omega_0/\omega$ from Eq. (67) for $|\omega_0/\omega| < \widetilde{R}_i \forall i$, one obtains the equations of the limit curve for interface motion in the $X^{\mathrm{a}}_n - X^{\mathrm{a}}_c$ plane (Fig. 4)

$$f_{\pm}(\overline{\boldsymbol{X}}^{\mathrm{a}}) := \pm X^{\mathrm{a}}_n - P\left[Q - \frac{1}{4P^2n}(\overline{X}^{\mathrm{a}}_c)^2\right] = 0. \tag{69}$$

The case $|\omega_0/\omega| > \widetilde{R}^{\mathrm{max}}_i$ yields just two corner points $\overline{\boldsymbol{X}}^{\mathrm{a}} = (0, \pm 2\overline{A})$, since they correspond to nonunique $\omega_0/\omega$. For $X^{\mathrm{a}}_n = 0$ one obtains $\overline{X}^{\mathrm{a}}_{cI} = 2P\sqrt{n\sum_{i=1}^n R_i^2}$ from Eq. (69) and $X^{\mathrm{a}}_{cII} = 2k\overline{R}\sum_{i=1}^n R_i/S$ from the equation $\overline{\boldsymbol{X}}^{\mathrm{a}} = (0, \pm 2\overline{A})$. Due to Cauchy–Bunyakovsky inequality $n\sum_{i=1}^n \widetilde{R}_i^2 \geqslant (\sum_{i=1}^n \widetilde{R}_i)^2$, one always has $\overline{X}^{\mathrm{a}}_{cI} \geqslant \overline{X}^{\mathrm{a}}_{cII}$, where equality holds for equal $R_i$. Thus, the point at the limit curve corresponding to $X^{\mathrm{a}}_n = 0$ is represented by the corner points $\overline{X}^{\mathrm{a}}_{cI} = \pm 2\overline{A}$ which for equal $R_i$ coincide with those found from Eq. (69).

An associated interface motion rule $\bar{\omega} = h\frac{\mathrm{d}f}{\mathrm{d}\boldsymbol{X}^{\mathrm{a}}}$ has the form

$$\omega_0 = h\frac{\partial f}{\partial \overline{X}^{\mathrm{a}}_c} = 0.5\frac{h}{Pn}\overline{X}^{\mathrm{a}}_c, \quad \omega = h\frac{\partial f}{\partial X^{\mathrm{a}}_n} = \pm h, \quad \frac{\omega_0}{\omega} = \pm\frac{0.5}{Pn}\overline{X}^{\mathrm{a}}_c = \pm\left(\frac{PQ \mp X^{\mathrm{a}}_n}{Pn}\right)^{0.5}, \tag{70}$$
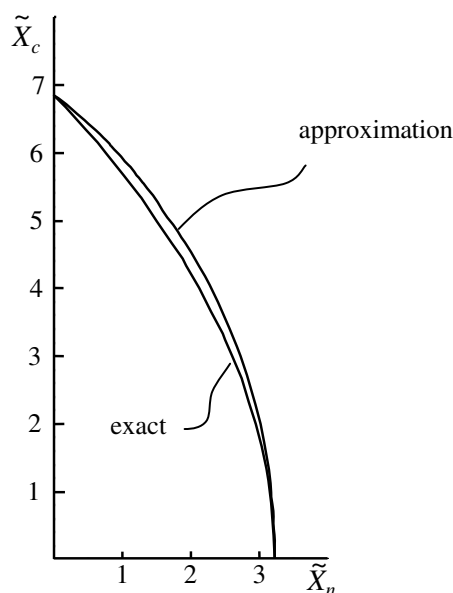


Fig. 4. Plots of the limit curves $f(\overline{X}^{\mathrm{a}}_c, X^{\mathrm{a}}_n) = 0$ for 5 interfaces ($n = 5$) with lengths $2R = 0.1, 0.4, 0.8, 1.0,$ and $1.4$ and $P = 1$ based on (a) exact Eq. (79) and (b) approximate Eq. (82).

where Eq. (69) has been used to express $\overline{X}_c^a$ in terms of $X_n^a$. At the singular points $X^a = (0, \pm 2\overline{A})$, where the normal is ambiguous, the vector $\bar{\omega}$ is a linear combination of the normals to the surfaces $f_+$ and $f_-$:

$$\omega_0 = h_1 \frac{\partial f_+}{\partial \overline{X}_c^a} + h_2 \frac{\partial f_-}{\partial \overline{X}_c^a} = \frac{0.5}{Pn}(h_1 + h_2)\overline{X}_c^a,$$

$$\omega = h_1 \frac{\partial f_+}{\partial X_n^a} + h_2 \frac{\partial f_-}{\partial X_n^a} = (h_1 - h_2), \tag{71}$$

$$\frac{\omega_0}{\omega} = \frac{0.5}{Pn}\frac{h_1 + h_2}{h_1 - h_2}\overline{X}_c^a = \frac{h_1 + h_2}{h_1 - h_2}\left(\frac{PQ \mp X_n^a}{Pn}\right)^{0.5},$$

where $h_1 > 0$ and $h_2 > 0$ are constants. The dissipative potential can be found in the way similar to single interface case:

$$\Psi(\overline{X}) = \frac{g_2}{3\overline{B}}\overline{X}_c + \frac{g_5 X_n}{g_4} - \frac{g_5^2 g_2 (1 + g_3)}{6g_4^2} - \frac{g_5 P(Q + ng_3/3)}{g_4} \quad \text{for } \overline{X}_c - \frac{3\overline{A}}{\overline{B}}\widetilde{R}_i \leqslant 2,$$

$$\Psi(\overline{X}) = \frac{(\overline{X}_c - 2\overline{A})^2 + 3X_n^2}{6\overline{B}} \quad \text{for } \overline{X}_c - \frac{3\overline{A}}{\overline{B}}R_i X_n > 2. \tag{72}$$

Here $g_1 = (9n^2 P^2 \overline{X}_c + (n^3 P^3(81nP\overline{X}_c^2 + 4(2nPQ + 3X_n)^3)))^1/2$, $g_2 = \overline{X}_c - \frac{2^{1/3}g_4}{3g_1^{1/3}}$, $g_3 = 3g_4^2/g_5^2$, $g_4 = -4n^2 P^2 + 6nP(PQ - X_n) + 2^{1/3}g_1^{1/3}$ and $g_5 = 2^{2/3}3nPg_1^{1/3}$. For $\overline{X}_c, X_n > 0$, $\bar{\omega} = \mathrm{d}\Psi/\mathrm{d}X$ is given by equations

$$\omega_0 = \frac{g_2}{3\overline{B}}, \quad \omega = \frac{g_2 g_5}{3\overline{B}g_4} \quad \text{for } \overline{X}_c - \frac{3\overline{A}}{\overline{B}}\widetilde{R}_i X_n \leqslant 2,$$

$$\omega_0 = \frac{\overline{X}_c - 2}{3\overline{A}}, \quad \omega = \frac{X_n}{\overline{B}} \quad \text{for } \overline{X}_c - \frac{3\overline{A}}{\overline{B}}R_i X_n > 2. \tag{73}$$

**Case 3.** We will consider the general case when the center of an interface rotation belongs to $m$ interfaces and is outside of other $n - m$ interfaces. Using the same calculations, we derive

$$\frac{D_a}{P} = |\omega|\left(\sum_{i=1}^m \widetilde{R}_i^2 + m\frac{\omega_0^2}{\omega^2}\right) + 2|\omega_0|\sum_{i=m+1}^n \widetilde{R}_i, \tag{74}$$

where for interfaces 1 to $m$ holds $|r_c| \leqslant R_i$ or $|\frac{\omega_0}{\omega}| \leqslant \widetilde{R}_i$ and for interfaces $m + 1$ to $n$ the opposite $|r_c| \geqslant R_i$ or $|\frac{\omega_0}{\omega}| \geqslant \widetilde{R}_i$ is true. The main problem in analyzing Eq. (74) and following from it equations is related to the fact that that $m$ depends on $\frac{\omega_0}{\omega}$ in a discontinuous way. The integer $m$ is constant when $|\frac{\omega_0}{\omega}|$ varies between any two nearest $\widetilde{R}_k$ and $\widetilde{R}_{k+1}$ and increases by 1 when it is getting outside the interval $[R_k, R_{k+1}]$. However, we will show below that the dissipation function (74) is not only continuous but also has continuous first derivatives, i.e. function $\overline{X}^a(\bar{\omega}) = \frac{\mathrm{d}D_a}{\mathrm{d}\bar{\omega}}$ and consequently the limit curve $f(\overline{X}^a) = 0$ are continuous as well. Indeed, for $\frac{\omega_0}{\omega} = \widetilde{R}_m$, one obtains from (74) for $m - 1$ interfaces

$$\frac{D_a^-}{P|\omega|} = \left( \sum_{i=1}^{m-1} \widetilde{R}_i^2 + (m-1)\widetilde{R}_m^2 \right) + 2\widetilde{R}_m \sum_{i=m}^{n} \widetilde{R}_i \tag{75}$$

and for $m$ interfaces

$$\frac{D_a^+}{P|\omega|} = \left( \sum_{i=1}^{m} \widetilde{R}_i^2 + m\widetilde{R}_m^2 \right) + 2\widetilde{R}_m \sum_{i=m+1}^{n} \widetilde{R}_i. \tag{76}$$

The first parenthesis in $D_a^+/(P|\omega|)$ is larger that one in $D_a^-/(P|\omega|)$ by $2\widetilde{R}_m^2$, while the second term in $D_a^+/(P|\omega|)$ is smaller that one in $D_a^-/(P|\omega|)$ by the same $2\widetilde{R}_m^2$, i.e. $D_a^- = D_a^+$. Then we obtain

$$\overline{X}_c^{a,m} = \frac{\partial D_a}{\partial \omega_0} = 2P\left( m\frac{\omega_0}{\omega} + \sum_{i=m+1}^{n} \widetilde{R}_i \right) \quad \text{for } \widetilde{R}_{m+1} \leqslant \frac{\omega_0}{\omega} \leqslant \widetilde{R}_m,$$

$$X_n^{a,m} = \frac{\partial D_a}{\partial \omega} = P\left( \sum_{i=1}^{m} \widetilde{R}_i^2 - m\frac{\omega_0^2}{\omega^2} \right) \quad \text{for } \widetilde{R}_{m+1} \leqslant \frac{\omega_0}{\omega} \leqslant \widetilde{R}_m, \tag{77}$$

$$\overline{X}_c^{v} = 0.5\frac{\partial D_v}{\partial \omega_0} = 3\overline{B}\omega_0, \quad X_n^{v} = 0.5\frac{\partial D_v}{\partial \omega} = \overline{B}\omega, \tag{78}$$

where superscript $m$ means the case when the center or rotation is located within $m$ interfaces. Eq. (77) have to be used for each $m$ separately in the range $\widetilde{R}_{m+1} \leqslant \omega_0/\omega \leqslant \widetilde{R}_m$; here we designate $\widetilde{R}_0 = \infty$ and $\widetilde{R}_{n+1} = 0$. Continuity of $\overline{X}^a(\bar{\omega})$ at the points $\omega_0/\omega = \widetilde{R}_m$ can be checked by direct calculations, similar to that for $D_a(\bar{\omega})$. Excluding $\omega_0/\omega$ from Eq. (77), we obtain explicit expression for the limit curve

$$f(\overline{X}_c^{a,m}, X_n^{a,m}) = X_n^{a,m} - P\left[ \sum_{i=1}^{m} \widetilde{R}_i^2 - \frac{1}{m}\left( \frac{\overline{X}_c^{a,m}}{2P} - \sum_{i=m+1}^{n} \widetilde{R}_i \right)^2 \right] = 0 \quad \text{for} \quad \widetilde{R}_{m+1} \leqslant \frac{\omega_0}{\omega} \leqslant \widetilde{R}_m. \tag{79}$$

For $X_c = 0$ one has $\omega_0 = 0$, $m = n$ and $X_n = PQ$ (like in Eq. (69)). For $X_n = 0$ one has $m = 0$ and $X_c = 2P\sum_{i=1}^{n} \widetilde{R}_i$. Plot of the limit curve $f(\overline{X}_c^a, X_n^a) = 0$ for $n = 5$ and some chosen values of $R_i$ is presented in Fig. 4.

The structure of the dissipative potential and the rates $\omega$ and $\omega_0$ become the same with the one for Case 2 if $n$ is substituted by $m$ (also $n$ in $Q$) and $\overline{X}_c$ by $\overline{X}_c - 2P\sum_{i=m+1}^{n} \widetilde{R}_i$ in Eqs. (72) and (73). Then the dissipative potential becomes

$$\Psi(\overline{X}) = \frac{g_2}{3\overline{B}}\left( \overline{X}_c - 2P\sum_{i=m+1}^{n} \widetilde{R}_i \right) + \frac{g_5 X_n}{g_4} - \frac{g_5^2 g_2 (1+g_3)}{6g_4^2} - \frac{g_5 P(Q+mg_3/3)}{g_4}$$

$$\text{for } \overline{X}_c - \frac{3\overline{A}}{\overline{B}}\widetilde{R}_i \leqslant 2 + 2P\sum_{i=m+1}^{n} \widetilde{R}_i; \Psi(\overline{X}) = \frac{\left( \left( \overline{X}_c - 2P\sum_{i=m+1}^{n} \widetilde{R}_i \right) - 2\overline{A} \right)^2 + 3X_n^2}{6\overline{B}}$$

$$\text{for } \overline{X}_c - \frac{3\overline{A}}{\overline{B}}\overline{R}_i X_n > 2 + 2P\sum_{i=m+1}^{n} \widetilde{R}_i, \tag{80}$$

where $\quad g_1 = [9m^2 P^2(\overline{X}_c - 2P\sum_{i=m+1}^{n} \widetilde{R}_i) + (m^3 P^3 (81mP(\overline{X}_c - 2P\sum_{i=m+1}^{n} \widetilde{R}_i) + 4(2mPQ + 3X_n)^3))]^{1/2}, \quad g_2 = (\overline{X}_c - 2P\sum_{i=m+1}^{n} \widetilde{R}_i) - \frac{2^{1/3}g_4}{3g_1^{1/3}}, \quad g_3 = 3g_4^2/g_5^2, \quad g_4 = -4m^2 P^2 + 6mP$

$(PQ - X_n) + 2^{1/3}g_1^{1/3}$ and $g_5 = 2^{2/3}3mPg_1^{1/3}$. For $\quad \overline{X}_c, X_n > 0$, $\bar{\omega} = \mathrm{d}\Psi/\mathrm{d}X$ is given by equations

$$\omega_0 = \frac{g_2}{3\overline{\overline{B}}}, \quad \omega = \frac{g_2 g_5}{3\overline{\overline{B}}g_4} \quad \text{for } \overline{X}_c - \frac{3\overline{A}}{\overline{B}}\widetilde{R}_i X_n \leqslant 2 + 2P\sum_{i=m+1}^{n}\widetilde{R}_i;$$

$$\omega_0 = \frac{\overline{X}_c - 2P\sum_{i=m+1}^{n}\widetilde{R}_i - 2}{3\overline{A}}, \quad \omega = \frac{X_n}{B} \quad \text{for } \overline{X}_c - \frac{3\overline{A}}{B}\overline{R}_i X_n > 2 + 2P\sum_{i=m+1}^{n}\widetilde{R}_i. \quad (81)$$

When there are too many interfaces, it becomes computationally time consuming to perform due to large amount of logical operators. One needs a simple expression which approximates the limit curve given by (79) by a single function. We will approximate Eq. (79) by Eq. (69) obtained for the Case 2 which is in the form $X_n = \eta_1 + \eta_2 \overline{X}_c^2$. Determining the coefficients $\eta_1$ and $\eta_2$ from the condition that Eq. (79) and (69) coincide for the points $X_c = 0$ and $X_n = 0$, one obtains $\eta_1 = PQ$ and $\eta_2 = -Q/(4P(\sum_{i=1}^{n}\widetilde{R}_i)^2)$, i.e.

$$f_{\pm}(\overline{X}^a) := \pm X_n^a - PQ\left(1 - \frac{1}{4P^2\left(\sum_{i=1}^{n}\widetilde{R}_i\right)^2}(\overline{X}_c^a)^2\right) = 0. \quad (82)$$

Plot of the exact Eq. (79) and approximated Eq. (82) limit curves for $n = 5$ and some chosen values of $R_i$ are presented in Fig. 4. Dissipative potential equation (80) and kinetic equation (81) change accordingly.

### 3.5. Additional geometric interpretation

For additional geometric interpretation, it is convenient to introduce one more function, namely $D_a(\boldsymbol{k}) := D_a(\bar{\omega})/|\bar{\omega}|$ (Levitas, 1995, 1996a), where $|\bar{\omega}|$ is the magnitude of the vector $\bar{\omega}$ and $\boldsymbol{k} := \bar{\omega}/|\bar{\omega}|$ is the unit vector along the $\bar{\omega}$. By definition of time-scale independent athermal force, $\overline{X}^a(\bar{\omega})$ is homogeneous functions of degree zero, i.e. $\overline{X}^a(\bar{\omega}) = \overline{X}^a(\boldsymbol{k})$. Then both $\overline{X}^a \cdot \bar{\omega} = |\bar{\omega}|X^a \cdot \boldsymbol{k}$ for a fixed $X^a$ and $D_a(\bar{\omega}) = |\bar{\omega}|D_a(\boldsymbol{k})$ are homogeneous functions of degree one. When varying all possible vectors $\boldsymbol{k} \in \mathscr{R}^2$, the ends of vectors $\overline{X}^a(\boldsymbol{k})$, corresponding to them, describe the limit curve for an interface motion $f(\overline{X}^a) = 0$, within which (i.e. for $f(\overline{X}^a) < 0$) we have $\bar{\omega} = 0$. It is evident that if for a given $\overline{X}^a$ an inequality

$$\overline{X}^a \cdot \bar{\omega} - D_a(\bar{\omega}) < 0 \quad \forall \bar{\omega} \neq 0 \quad (83)$$

is valid, then for this $\overline{X}^a$ one has $\bar{\omega} = \boldsymbol{0}$. Indeed, if $\bar{\omega} \neq \boldsymbol{0}$, then for this $\bar{\omega}$ and corresponding to it $\overline{X}^a = \overline{X}^a(\bar{\omega})$ one has $\overline{X}^a \cdot \bar{\omega} = D_a(\bar{\omega})$, which is in contradiction with inequality (83). Since $\overline{X}^a \cdot \bar{\omega} - D_a(\bar{\omega}) = |\bar{\omega}|(\overline{X}^a \cdot \boldsymbol{k} - D_a(\boldsymbol{k}))$, then inequality (83) can be presented in an equivalent form $\overline{X}^a \cdot \boldsymbol{k} - D_a(\boldsymbol{k}) < 0, \forall \boldsymbol{k} \in \mathscr{R}^2$. In a geometric interpretation this means that the circle $\overline{X}^a \cdot \boldsymbol{k}$, plotted on vector $\overline{X}^a$ as on the diameter, is inside the curve $D_a(\boldsymbol{k})$ that characterizes an athermal resistance to motion in direction $\boldsymbol{k}$ (Fig. 5). The condition $X^a \cdot \boldsymbol{k} - D_a(\boldsymbol{k}) = 0$ could be fulfilled when the circle $X^a \cdot \boldsymbol{k}$ and the curve $D_a(\boldsymbol{k})$ have the common points, i.e. at their intersection or touching. Touching is the first possibility to meet the condition for the interface motion and according the postulate of realizability (Levitas, 1995) we assume, that this possibility is realized, i.e. $\bar{\omega} \neq 0$. Vector $\bar{\omega}$ may be directed to the touching point only, because for any other direction $\boldsymbol{k}$ we have
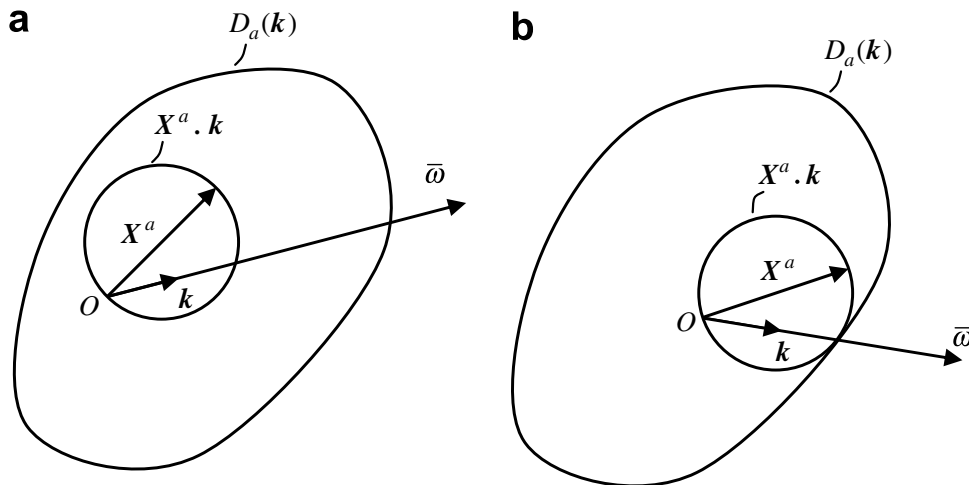
Fig. 5. Geometric interpretation of the phase transformation criterion using curve $D_a(\boldsymbol{k})$ that characterizes an athermal resistance to interface motion in direction $\boldsymbol{k}$. (a) When the circle $\overline{X}^{\mathrm{a}} \cdot \boldsymbol{k}$, plotted on vector $\overline{X}^{\mathrm{a}}$ as on the diameter, is inside the curve $D_a(\boldsymbol{k})$, the interface motion cannot occur. (b) When these curves touch, the interface motion occurs according the postulate of realizability (Levitas, 1995).

$\overline{X}^{\mathrm{a}} \cdot \boldsymbol{k} - D_{\mathrm{a}}(\boldsymbol{k}) < 0$ (Fig. 5). This assumption leads to the normality rule $\overline{X}^{\mathrm{a}} = \frac{\mathrm{d}D_{\mathrm{a}}}{\mathrm{d}\bar{\omega}}$ (which coincides with Eq. (49) for $z = 1$) and followed from it associated interface motion rule (53) (Levitas, 1995, 1996a) and all their particular cases that we already discussed. In a geometric interpretation, the postulate of realizability means that if in the course of the variation of $\overline{X}^{\mathrm{a}}$ the circle $\overline{X}^{\mathrm{a}} \cdot \boldsymbol{k}$ and the curve $D_{\mathrm{a}}(\boldsymbol{k})$ touch for the first time, then $\quad \bar{\omega} \neq \boldsymbol{0}$. Vector $\boldsymbol{k}$ can be characterized by an angle $\alpha$ between the vector $\bar{\omega}$ and horizontal axis $\omega$. Focusing on $0 \leqslant \alpha \leqslant \pi/2$, one expresses Eq. (45) for single interface in the form
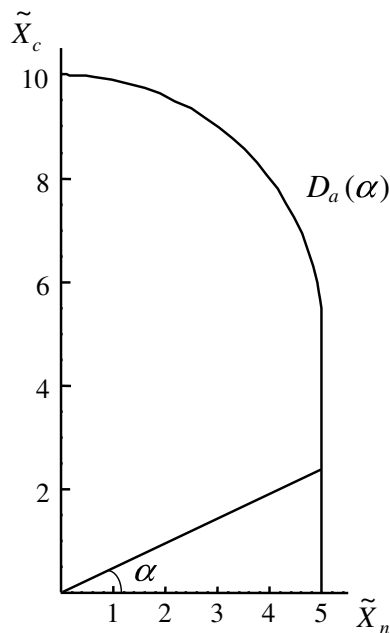


Fig. 6. Plot of the function $D_{\mathrm{a}}(\alpha)$ for single interface - vertical line for $0 \leqslant \alpha \leqslant \pi/4$ and quarter of a circle for $\pi/4 \leqslant \alpha \leqslant \pi/2$.

$$D_a(\alpha) := \frac{D_a}{|\bar{\omega}|} = A\cos(\alpha)(1 + \tan^2(\alpha)) = \frac{A}{\cos(\alpha)} \quad \text{for } 0 \leqslant \alpha \leqslant \pi/4, \tag{84}$$

$$D_a(\alpha) = 2A\sin(\alpha) \quad \text{for } \pi/4 \leqslant \alpha \leqslant \pi/2. \tag{85}$$

This curve is presented in Fig. 6 and consists of vertical line for $0 \leqslant \alpha \leqslant \pi/4$ and quarter of a circle for $\pi/4 \leqslant \alpha \leqslant \pi/2$. Since the circle $\overline{X}^a \cdot k$ for the vertical $\overline{X}^a$ is $|\overline{X}^a|\sin(\alpha)$, it coincides for $X_c^a = 2A$ with the quarter of the circle Eq. (85) for $\pi/4 \leqslant \alpha \leqslant \pi/2$. This means that for this $\overline{X}^a$ the vector $\bar{\omega}$ is arbitrary directed within $\pi/4 \leqslant \alpha \leqslant \pi/2$ which corresponds to a corner point at the limit curve $f(\overline{X}^a) = 0$.

For multiple-interface case, we obtain from Eq. (74)

$$D_a(\alpha)/P = m\cos(\alpha)\left(\frac{1}{m}\sum_{i=1}^{m}\widetilde{R}_i^2 + \tan^2(\alpha)\right) + 2\sin(\alpha)\sum_{i=m+1}^{n}\widetilde{R}_i, \tag{86}$$

where $\widetilde{R}_i := R_i/\overline{R}$. We obtain that $D_a(0) = P\sum_{i=1}^{n}\widetilde{R}_i^2$ (since $m = n$) and $D_a(\pi/2) = 2P\sum_{i=1}^{n}\widetilde{R}_i$ (since $m = 0$). Plot of the function $D_a(\alpha)$ for $n = 5$ and some chosen values of $R_i$ is presented in Fig. 7.

## 4. Strains and stresses in phases. Driving forces for martensite I–martensite II interfaces

### 4.1. Two-phase system

When there are two phases, 1 and 2 (Fig. 1a), by inserting the strains $\varepsilon_1$, and $\varepsilon_2$ obtained from Eq. (9)$_1$, into Eq. (1) we obtain for the prescribed strain $\varepsilon$

$$\varepsilon_1 = \varepsilon - c_2(an)_s, \quad \varepsilon_2 = \varepsilon + c_1(an)_s. \tag{87}$$

By using Eq. (87) and Hooke's law, Eq. (9)$_2$ is expressed as

$$n \cdot E_1 : (\varepsilon - c_2(an)_s) = n \cdot E_2 : (\varepsilon + c_1(an)_s - \varepsilon_{t2}). \tag{88}$$
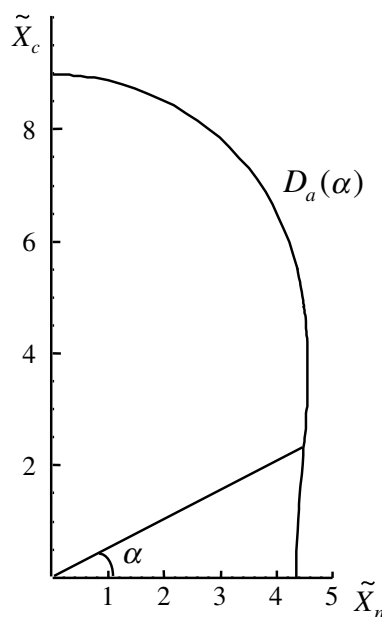


Fig. 7. Plot of the function $D_a(\alpha)$ for 5 interfaces with lengths $2R = 0.6, 0.8, 1.0, 1.2, 1.4$.

By solving this linear equation, the vector $\boldsymbol{a}$ is obtained. Inserting $\boldsymbol{a}$ into Eq. (87), the strains in each phase, $\boldsymbol{\varepsilon}_1$ and $\boldsymbol{\varepsilon}_2$, are found. Then, using Hooke's law, stresses in each phase $\boldsymbol{\sigma}_1$ and $\boldsymbol{\sigma}_2$ are obtained, i.e.

$$\boldsymbol{\sigma}_1 = \boldsymbol{E}_1 : (\boldsymbol{\varepsilon} - c_2(\boldsymbol{an})_s), \quad \boldsymbol{\sigma}_2 = \boldsymbol{E}_2 : (\boldsymbol{\varepsilon} + c_1(\boldsymbol{an})_s - \boldsymbol{\varepsilon}_{t2}). \tag{89}$$

Then Eq. (2) gives us the macroscopic stress. Macroscopic transformation strain is determined by equation

$$\boldsymbol{\varepsilon}^t = c_1 \boldsymbol{\varepsilon}_1^t : \boldsymbol{B}_1 + c_2 \boldsymbol{\varepsilon}_2^t : \boldsymbol{B}_2, \tag{90}$$

where $\boldsymbol{B}_i$ are the fourth-rank stress concentration tensors that connect $\boldsymbol{\sigma}_i$ and $\boldsymbol{\sigma}$ for the case without transformation strain: $\boldsymbol{\sigma}_i = \boldsymbol{B}_i : \boldsymbol{\sigma}$. Explicit expression for $\boldsymbol{B}_i$ for laminate structure of interest can be found in Stupkiewicz and Petryk (2002). For equal elastic moduli, $\boldsymbol{B}_i$ are identity tensors and $\boldsymbol{\varepsilon}^t = c_1 \boldsymbol{\varepsilon}_1^t + c_2 \boldsymbol{\varepsilon}_2^t$. For austenite, $\boldsymbol{\varepsilon}_1^t = 0$. Since $\boldsymbol{\varepsilon}_i^t$ are given and are constant, one does not need an additional "flow" rule for $\boldsymbol{\varepsilon}^t$: tensor $\boldsymbol{\varepsilon}^t$ can be found after integration of kinetic equation for concentration $c_2$. Note that knowledge of $\boldsymbol{\varepsilon}^t$ is not necessary for completing of the system of equation for the description of the coupled evolution of the microstructure and stress–strain state.

### 4.2. Three-phase system

Here we consider the volume $V$, consisting of austenite (A) and martensite (M), divided by a plane interface (or multiple plane parallel interfaces), see Fig. 1b–d. Martensite itself consists of the fine mixture of two martensitic variants which we will designate $M_I$ and $M_{II}$ (Fig. 1b–d). We first apply the above equations to the two-phase system $M_I$–$M_{II}$, and find average stresses, and strains, and effective properties of martensite mixture. Then, we consider in the same way the two phase austenite–martensite system. The traction continuity and Hadamard compatibility conditions for A–M and $M_I$–$M_{II}$ interfaces are

$$\begin{aligned}\boldsymbol{\sigma}_A \cdot \boldsymbol{n} &= \boldsymbol{\sigma}_M \cdot \boldsymbol{n}, \quad \boldsymbol{\sigma}_I \cdot \boldsymbol{n}_I = \boldsymbol{\sigma}_{II} \cdot \boldsymbol{n}_I, \\ \boldsymbol{\varepsilon}_M - \boldsymbol{\varepsilon}_A &= (\boldsymbol{an})_s, \quad \boldsymbol{\varepsilon}_{II} - \boldsymbol{\varepsilon}_I = (\boldsymbol{a}_I \boldsymbol{n}_I)_s,\end{aligned} \tag{91}$$

where the vectors $\boldsymbol{a}$ and $\boldsymbol{a}_I$ characterize the strain jumps across the A–M and $M_I$–$M_{II}$ interfaces. Dissipation rate per unit volume $V$ can be reduced to the form

$$D_V = X_c \dot{c}_M + X_c^1 \dot{c}_{II} + \boldsymbol{X}_n \cdot \dot{\boldsymbol{n}} + \boldsymbol{X}_n^I \cdot \dot{\boldsymbol{n}}_I \geqslant 0. \tag{92}$$

Here,

$$X_c = 0.5(\boldsymbol{\sigma}_A + \boldsymbol{\sigma}_M) : \boldsymbol{\varepsilon}_M^t - \boldsymbol{\varepsilon}_A^e : (\boldsymbol{E}_M - \boldsymbol{E}_A) : \boldsymbol{\varepsilon}_M^e - (\psi_M^\theta - \psi_A^\theta) \tag{93}$$

is the driving force for A–M transformation ($\boldsymbol{\varepsilon}_A^t = 0$), where $\boldsymbol{E}_M$ is the effective elastic modulus of the $M_I + M_{II}$ mixture and

$$\boldsymbol{\varepsilon}^t = \frac{c_I}{c_M} \boldsymbol{\varepsilon}_I^t : \boldsymbol{B}_I + \frac{c_{II}}{c_M} \boldsymbol{\varepsilon}_{II}^t : \boldsymbol{B}_{II} \tag{94}$$

is the transformation strain averaged over martensitic volume. Here $\frac{c_I}{c_M}$ and $\frac{c_{II}}{c_M}$ are the volume fractions of $M_i$ variant in $M_I + M_{II}$ mixture, $\boldsymbol{B}_I$ and $\boldsymbol{B}_{II}$ are the fourth-rank stress concentration tensors that linearly connect $\boldsymbol{\sigma}_I$ and $\boldsymbol{\sigma}_{II}$ with $\boldsymbol{\sigma}_M$ for the case without transformation strain. Explicit expressions for $\boldsymbol{B}_I$, $\boldsymbol{B}_{II}$ and $\boldsymbol{E}_M$ for laminate structure

can be found in Stupkiewicz and Petryk (2002). For equal elastic moduli of martensitic variants, we obtain

$$\varepsilon_{M}^{t} = \frac{c_{I}}{c_{M}} \varepsilon_{I}^{t} + \frac{c_{II}}{c_{M}} \varepsilon_{II}^{t}. \tag{95}$$

In our simulations in Part II, we use Eq. (95). Since $c_{I}$ and $c_{II}$ are determined by kinetic equations, we do not need an additional "flow" rule for $\varepsilon_{M}^{t}$. Also,

$$X_{c}^{I} := 0.5(\boldsymbol{\sigma}_{I} + \boldsymbol{\sigma}_{II}) : (\boldsymbol{\varepsilon}_{tI} - \boldsymbol{\varepsilon}_{tII}) - \boldsymbol{\varepsilon}_{I}^{e} : (\boldsymbol{E}_{II} - \boldsymbol{E}_{I}) : \boldsymbol{\varepsilon}_{II}^{e} \tag{96}$$

is the driving force for the $M_{I}$–$M_{II}$ transformation and

$$\boldsymbol{X}_{n} := -c_{A}c_{M}\boldsymbol{a} \cdot (\boldsymbol{\sigma}_{M} - \boldsymbol{\sigma}_{A}) \quad \text{and} \quad \boldsymbol{X}_{n}^{I} := -c_{I}c_{II}\boldsymbol{a}_{I} \cdot (\boldsymbol{\sigma}_{II} - \boldsymbol{\sigma}_{I}) \tag{97}$$

are the expressions for the thermodynamic driving forces for interface rotation for A–M and $M_{I}$–$M_{II}$ interfaces, respectively. If the difference in elastic moduli for the phases is negligible, the second terms in these equations disappear.

For the strains in austenite and martensite phases, we obtain

$$\boldsymbol{\varepsilon}_{A} = \boldsymbol{\varepsilon} - c_{M}(\boldsymbol{an})_{s}, \quad \boldsymbol{\varepsilon}_{M} = \boldsymbol{\varepsilon} + c_{A}(\boldsymbol{an})_{s}. \tag{98}$$

Then, using Eq. (98) and the equation for strain in martensite $\varepsilon_{M} = \frac{c_{I}}{c_{M}} \varepsilon_{I} + \frac{c_{II}}{c_{M}} \varepsilon_{II}$, $\varepsilon_{I}$ and $\varepsilon_{II}$ are expressed as

$$\begin{aligned} \boldsymbol{\varepsilon}_{I} &= \boldsymbol{\varepsilon} + c_{A}(\boldsymbol{an})_{s} - c_{II}/c_{M}(\boldsymbol{a}_{I}\boldsymbol{n}_{I})_{s}, \\ \boldsymbol{\varepsilon}_{II} &= \boldsymbol{\varepsilon} + c_{A}(\boldsymbol{an})_{s} + c_{I}/c_{M}(\boldsymbol{a}_{I}\boldsymbol{n}_{I})_{s}. \end{aligned} \tag{99}$$

Inserting Eqs. (98) and (99) and Hooke's laws into Eq. (91)$_1$ and (91)$_2$ results in

$$\boldsymbol{n} \cdot \boldsymbol{E}_{A} : (\boldsymbol{\varepsilon} - c_{M}(\boldsymbol{an})_{s}) = \boldsymbol{n} \cdot \boldsymbol{E}_{M} : (\boldsymbol{\varepsilon} + c_{A}(\boldsymbol{an})_{s} - \boldsymbol{\varepsilon}_{tM}), \tag{100}$$

$$\begin{aligned} \boldsymbol{n}_{I} \cdot \boldsymbol{E}_{I} : (\boldsymbol{\varepsilon} + c_{A}(\boldsymbol{an})_{s} - c_{II}/c_{M}(\boldsymbol{a}_{I}\boldsymbol{n}_{I})_{s} - \boldsymbol{\varepsilon}_{tI}) &= \boldsymbol{n}_{I} \cdot \boldsymbol{E}_{II} : (\boldsymbol{\varepsilon} + c_{A}(\boldsymbol{an})_{s} \\ &+ c_{I}/c_{M}(\boldsymbol{a}_{I}\boldsymbol{n}_{I})_{s} - \boldsymbol{\varepsilon}_{tII}). \end{aligned} \tag{101}$$

From these two independent linear vector equations, the vectors characterizing the jumps in strains $\boldsymbol{a}$ and $\boldsymbol{a}_{I}$ are found for prescribed strains $\boldsymbol{\varepsilon}$. Inserting $\boldsymbol{a}$ and $\boldsymbol{a}_{I}$ into Eqs. (99) and (98), the strains in martensitic variants and each phase $\varepsilon_{I}$, $\varepsilon_{II}$, $\varepsilon_{A}$ and $\varepsilon_{M}$ are found. Then, using Hooke's law, stresses in martensitic variants and each phase $\boldsymbol{\sigma}_{A}$, $\boldsymbol{\sigma}_{M}$, $\boldsymbol{\sigma}_{I}$ and $\boldsymbol{\sigma}_{II}$ are obtained:

$$\boldsymbol{\sigma}_{A} = \boldsymbol{E}_{A} : (\boldsymbol{\varepsilon} - c_{M}(\boldsymbol{an})_{s}), \tag{102}$$

$$\boldsymbol{\sigma}_{M} = \boldsymbol{E}_{M} : (\boldsymbol{\varepsilon} + c_{A}(\boldsymbol{an})_{s} - \boldsymbol{\varepsilon}_{tM}), \tag{103}$$

$$\boldsymbol{\sigma}_{I} = \boldsymbol{E}_{I} : (\boldsymbol{\varepsilon} + c_{A}(\boldsymbol{an})_{s} - c_{II}/c_{M}(\boldsymbol{a}_{I}\boldsymbol{n}_{I})_{s} - \boldsymbol{\varepsilon}_{tI}), \tag{104}$$

$$\boldsymbol{\sigma}_{II} = \boldsymbol{E}_{II} : (\boldsymbol{\varepsilon} + c_{A}(\boldsymbol{an})_{s} + c_{I}/c_{M}(\boldsymbol{a}_{I}\boldsymbol{n}_{I})_{s} - \boldsymbol{\varepsilon}_{tII}). \tag{105}$$

Averaging of $\boldsymbol{\sigma}_{A}$ and $\boldsymbol{\sigma}_{M}$ over the volume $V$ using Eq. (2) results in the macroscopic stress $\boldsymbol{\sigma}$.

Macroscopic transformation strain is determined by equation

$$\boldsymbol{\varepsilon}^{t} = c_{M}\boldsymbol{\varepsilon}_{M}^{t} : \boldsymbol{B}_{M}, \tag{106}$$

where $\boldsymbol{B}_{M}$ is the fourth-rank stress concentration tensor determined from $\boldsymbol{\sigma}_{M} = \boldsymbol{B}_{M} : \boldsymbol{\sigma}$. Again, $\boldsymbol{\varepsilon}^{t}$ can be found after integration of kinetic equation for concentrations $c_{I}$ and $c_{II}$ without an additional "flow" rule. Since knowledge of $\boldsymbol{\varepsilon}^{t}$ is not necessary for completing

of the system of equation for the description of the coupled evolution of the microstructure and stress–strain state, we do not determine it in our simulations.

### 4.3. Alternative expressions

Stresses and strains in phases can be found explicitly in the general matrix form, which is done for example in Levitas (1992), Stupkiewicz and Petryk (2002) and Levitas et al. (2004). We do not use these expressions in our computations because the approach described in Sections 4.1 and 4.2 is more effective computationally. However, in order to obtain some analytical solutions, and a general understanding of the parameters controlling internal stresses, it is desirable to obtain explicit equations for stresses and strains in phases. The most explicit equations obtained for the two-phase layered system with different anisotropic elastic moduli, presented in Stupkiewicz and Petryk (2002), are too bulky for analysis. Here, we derive equations for stresses and strains in phases for the case of equal elastic moduli in the form that allows transparent analysis. We will use our preliminary results from Levitas et al. (2004).

Let the axis 3 of the local orthogonal coordinate system be normal to the A–M interface. Here, we will use matrix notations for stress and strain tensors and elasticity tensors. We divide the six components of the stress tensor into two vectors: $\boldsymbol{\sigma}^{\perp} = (\sigma_{13}, \sigma_{23}, \sigma_{33})$, which contains the components normal to the A–M interface, and $\boldsymbol{\sigma}^{\parallel} = (\sigma_{11}, \sigma_{12}, \sigma_{22})$, which contains the in-layer components of the stress. The same is done for $\boldsymbol{\varepsilon}$ and $\boldsymbol{\varepsilon}_t$: $\boldsymbol{\varepsilon}^{\perp} = (2\varepsilon_{13}, 2\varepsilon_{23}, \varepsilon_{33})$, $\boldsymbol{\varepsilon}^{\parallel} = (\varepsilon_{11}, 2\varepsilon_{12}, \varepsilon_{22})$, $\boldsymbol{\varepsilon}_t^{\perp} = (2\varepsilon_{13}^t, 2\varepsilon_{23}^t, \varepsilon_{33}^t)$, and $\boldsymbol{\varepsilon}_t^{\parallel} = (\varepsilon_{11}^t, 2\varepsilon_{12}^t, \varepsilon_{22}^t)$. Stresses and strains in phases can be presented as the sum of internal and external (due to applied stresses or strains) contributions. For equal elastic moduli, the external stresses and strains in phases are equal to applied external stresses and strains, i.e.

$$\boldsymbol{\sigma}_1^{\mathrm{ex}} = \boldsymbol{\sigma}_2^{\mathrm{ex}} = \boldsymbol{\sigma}^{\mathrm{ex}} = \boldsymbol{E}\boldsymbol{\varepsilon}^{\mathrm{ex}}, \quad \boldsymbol{\varepsilon}_1^{\mathrm{ex}} = \boldsymbol{\varepsilon}_2^{\mathrm{ex}} = \boldsymbol{\varepsilon}^{\mathrm{ex}} = \boldsymbol{E}^{-1}\boldsymbol{\sigma}^{\mathrm{ex}}, \tag{107}$$

where $\boldsymbol{E}$ is the matrix of elastic moduli. Also, the transformation strain for the composite is equal to the volume averaged of transformation strains in the layers, $\boldsymbol{\varepsilon}^t = c_1\boldsymbol{\varepsilon}_1^t + c_2\boldsymbol{\varepsilon}_2^t$ and $\boldsymbol{\varepsilon} = \boldsymbol{\varepsilon}^t + \boldsymbol{\varepsilon}^{\mathrm{ex}}$. Thus, we can focus on internal stresses and strain. Hooke's law for each layer is

$$\begin{pmatrix} \boldsymbol{\sigma}_1^{\parallel\mathrm{in}} \\ \boldsymbol{\sigma}_1^{\perp\mathrm{in}} \end{pmatrix} = \begin{pmatrix} \boldsymbol{E}_{\parallel} & \boldsymbol{E}_{\square} \\ \boldsymbol{E}_{\square}^t & \boldsymbol{E}_{\perp} \end{pmatrix} \begin{pmatrix} \boldsymbol{\varepsilon}_1^{\parallel\mathrm{in}} - \boldsymbol{\varepsilon}_{t1}^{\parallel} \\ \boldsymbol{\varepsilon}_1^{\perp\mathrm{in}} - \boldsymbol{\varepsilon}_{t1}^{\perp} \end{pmatrix},$$

$$\begin{pmatrix} \boldsymbol{\sigma}_2^{\parallel\mathrm{in}} \\ \boldsymbol{\sigma}_2^{\perp\mathrm{in}} \end{pmatrix} = \begin{pmatrix} \boldsymbol{E}_{\parallel} & \boldsymbol{E}_{\square} \\ \boldsymbol{E}_{\square}^t & \boldsymbol{E}_{\perp} \end{pmatrix} \begin{pmatrix} \boldsymbol{\varepsilon}_2^{\parallel\mathrm{in}} - \boldsymbol{\varepsilon}_{t2}^{\parallel} \\ \boldsymbol{\varepsilon}_2^{\perp\mathrm{in}} - \boldsymbol{\varepsilon}_{t2}^{\perp} \end{pmatrix}, \tag{108}$$

where $\boldsymbol{E}_{\parallel}$, $\boldsymbol{E}_{\perp}$ and $\boldsymbol{E}_{\square}$ are the corresponding matrix parts of the elasticity matrix $\boldsymbol{E}$ and the superscript 't' denotes transposition. The homogeneous internal stress and strain in each phase satisfies the equilibrium and strain compatibility equations. Continuity of normal stresses and tangential displacements across the interface and zero averaged stress result in:

$$\boldsymbol{\sigma}_1^{\perp\mathrm{in}} = \boldsymbol{\sigma}_2^{\perp\mathrm{in}} = 0, \quad \boldsymbol{\varepsilon}_1^{\parallel\mathrm{in}} = \boldsymbol{\varepsilon}_2^{\parallel\mathrm{in}} \quad \text{and} \quad c_1\boldsymbol{\sigma}_1^{\parallel\mathrm{in}} + c_2\boldsymbol{\sigma}_2^{\parallel\mathrm{in}} = 0. \tag{109}$$

By solving Eqs. (108) and (109), we obtain for the elastic internal strain in each layer

$$\varepsilon_1^{\perp\,\mathrm{in}} - \varepsilon_{t1}^{\perp} = c_2 E_{\perp}^{-1} E_{\square}^{t} \Delta\varepsilon_t^{\|}, \quad \varepsilon_1^{\|\,\mathrm{in}} - \varepsilon_{t1}^{\|} = -c_2 \Delta\varepsilon_t^{\|},$$

$$\varepsilon_2^{\perp\,\mathrm{in}} - \varepsilon_{t2}^{\perp} = -c_1 E_{\perp}^{-1} E_{\square}^{t} \Delta\varepsilon_t^{\|}, \quad \varepsilon_2^{\|\,\mathrm{in}} - \varepsilon_{t2}^{\|} = c_1 \Delta\varepsilon_t^{\|}, \tag{110}$$

where $\Delta\varepsilon_t^{\|} = \varepsilon_{t1}^{\|} - \varepsilon_{t2}^{\|}$. Substituting Eq. (110) into Eq. (108), we obtain explicit expression for internal stresses

$$\begin{pmatrix} \sigma_1^{\|\,\mathrm{in}} \\ \sigma_1^{\perp\,\mathrm{in}} \end{pmatrix} = c_2 \begin{pmatrix} E_{\|} & E_{\square} \\ E_{\square}^{t} & E_{\perp} \end{pmatrix} \begin{pmatrix} -\Delta\varepsilon_t^{\|} \\ E_{\perp}^{-1} E_{\square}^{t} \Delta\varepsilon_t^{\|} \end{pmatrix},$$

$$\begin{pmatrix} \sigma_2^{\|\,\mathrm{in}} \\ \sigma_2^{\perp\,\mathrm{in}} \end{pmatrix} = -c_1 \begin{pmatrix} E_{\|} & E_{\square} \\ E_{\square}^{t} & E_{\perp} \end{pmatrix} \begin{pmatrix} -\Delta\varepsilon_t^{\|} \\ E_{\perp}^{-1} E_{\square}^{t} \Delta\varepsilon_t^{\|} \end{pmatrix}. \tag{111}$$

One of the results is that the jump in-layer part of the transformation strain only produces internal stresses. Jumps in normal components of the transformation strain do not contribute to Eq. (111), which is intuitively clear even for different elastic moduli of phases. Another result is that internal in-layer elastic strains are independent of elastic properties. Also, according to Eq. (110), the total internal strain is

$$\varepsilon^{\mathrm{in}} = c_1 \varepsilon_1^{\mathrm{in}} + c_2 \varepsilon_2^{\mathrm{in}} = c_1 \varepsilon_{1t} + c_2 \varepsilon_{2t} = \varepsilon_t. \tag{112}$$

Equations outlined in this subsection have been used to obtain analytical solutions for stress-induced normal reorientation in Part 2 of this paper.

## 5. Interface orientation and internal structure of an embryo

If one starts with a single phase material, nucleation of the product phase must be considered. We will not discuss here actual nucleation mechanisms that require consideration at the nanoscale or the consideration of specific nucleation sites with corresponding stress concentration and surface energy. Theory of heterogeneous martensite nucleation (Olson and Cohen, 1986; Olson and Roytburd, 1995) in which they suggested the existence of an embryo of the product phase stabilized by the stress field of the defects, even in the region of stability of the parent phase. We will also assume the existence of an embryo even for the negative driving force of the transformation $X_c$. In doing so, we will consider two cases.

In the first case, we will introduce a small embryo with a plane interface near a corner of the parallelepiped or two plane interfaces which possesses minimum Gibbs energy under the prescribed stress $\boldsymbol{\sigma}$. That means the orientation of its interface is determined by the orientational equilibrium condition $X_n = 0$. If the embryo represents a mixture of two martensitic variants, then two additional thermodynamic equilibrium equations must be added. The first equation added is for the orientation of the interfaces between variants $X_n^{\mathrm{I}} = 0$. The second equation is for the driving force of the variant–variant transformation $X_c^{\mathrm{I}} = 0$. These conditions guarantee the stationary rather than the minimum value of the Gibbs energy. In order to be sure this value corresponds to the minimum, we will apply permanently small perturbations and solve for $c = \mathrm{const}$ the simplest versions of the kinetic equations (26)

$$\dot{c}_{\mathrm{I}} = h_{cI} X_c^{\mathrm{I}}, \quad \dot{\boldsymbol{n}} = h_n X_n, \quad \dot{\boldsymbol{n}}_{\mathrm{I}} = h_{nI} X_n^{\mathrm{I}} \tag{113}$$

until the stationary solution is reached.

In the second case, an embryo may possess normal $n$, normal $n_I$ (for martensite–martensite mixture), and volume fractions of martensitic variants that do not correspond to the minimum of the Gibbs energy and zero driving forces. Since nucleation occurs in the stress fields of some defects, the sum of the applied stress and the stress field of the defect have to satisfy the conditions $X_n = 0$, $X_n^I = 0$ and $X_c^I = 0$. Thus, parameters of the embryo that do not correspond to the minimum of the Gibbs energy under prescribed external stresses mimic the presence of a stress field of the nucleating defect.

The phase transformation criterion is $X_c > 0$ in the absence of the athermal friction and $X_c > q(X_n)$ (see Eq. (79)) when the athermal friction is taken into account. When the phase transformation criterion is satisfied, the embryo transforms to an actual nucleus and starts to grow and evolve according to kinetic equations. When the nucleus grows away from the defect, the effect of the nucleating defect becomes negligible. Therefore, as soon as the transformation criterion is satisfied, nonzero thermodynamic forces $X_n$, $X_n^I$ and $X_c^I$ will cause the evolution of the system toward the equilibrium microstructure.

## 6. Thermodynamic driving force for interface reorientation at finite strains

We will derive the universal driving force for interface rotation for finite strains using the same parallelepiped $V$ in the reference (undeformed) configuration containing two phases, 1 and 2, divided by a plane interface $\Sigma$ with the unit normal $n$ under external stresses (Fig. 1). Let $F_i$ and $P_i$ be the deformation gradient and nonsymmetric Piola–Kirchoff stress tensors (the force per unit area in the undeformed state) in each phase, then we have the following relations for the macroscopic variables for the volume $V$

$$F = c_1 F_1 + c_2 F_2, \quad P = c_1 P_1 + c_2 P_2, \tag{114}$$

where $c_i := V_i/V$ is the volume fraction of the $i$th phase in the reference configuration, and $V_i$ is the volume of the $i$th phase. To derive the rate equation for the macroscopic free energy per unit mass $\psi$, it is convenient to introduce mass fractions of phases $c_i^m$ ($c_1^m + c_2^m = 1$). We obtain

$$c_i^m = \frac{m_i}{m} = \frac{\rho_i V_i}{\rho V} = \frac{\rho_i}{\rho} c_i \quad \text{and} \quad \dot{c}_i^m = \frac{\rho_i}{\rho} \dot{c}_i, \tag{115}$$

where $m_i$ and $m = m_1 + m_2$ are the mass of each phase and the entire volume $V$, $\rho_i$ and $\rho$ are the mass densities of each phase and the entire volume $V$ in the reference configuration. Then we can derive

$$\psi = c_1^m \psi_1 + c_2^m \psi_2, \quad \rho \psi = c_1 \rho_1 \psi_1 + c_2 \rho_2 \psi_2. \tag{116}$$

Differentiating the first Eq. (116), we obtain

$$\dot{\psi} = c_1^m \dot{\psi}_1 + c_2^m \dot{\psi}_2 + (\psi_2 - \psi_1)\dot{c}_2^m \quad \text{and} \quad \rho \dot{\psi} = c_1 \rho_1 \dot{\psi}_1 + c_2 \rho_2 \dot{\psi}_2 + \rho_2 [\psi]\dot{c}. \tag{117}$$

For simplicity, we will consider isothermal processes since allowing for variation in temperature does not lead to any changes in the driving forces for the interface propagation and reorientation. Also, the equation for entropy is the same as for small strains. The dissipation rate per unit total volume of each phase is

$$D_{Vi} = P_i^t : \dot{F}_i - \rho_i \dot{\psi}_i \geqslant 0. \tag{118}$$

Since $\psi_i = \psi_i(\mathbf{F}_i)$, then $D_i = (\mathbf{P}_i^t - \rho_i \frac{\partial \psi_i}{\partial \mathbf{F}_i^t}) : \dot{\mathbf{F}}_i = 0$ and $\mathbf{P}_i = \rho_i \frac{\partial \psi_i}{\partial \mathbf{F}_i}$. The dissipation rate per unit total volume is

$$D_V = \mathbf{P}^t : \dot{\mathbf{F}} - \rho \dot{\psi} \geqslant 0. \tag{119}$$

Substituting $\dot{\mathbf{F}} = c_1 \dot{\mathbf{F}}_1 + c_2 \dot{\mathbf{F}}_2 + [\mathbf{F}]\dot{c}$ and $\rho \dot{\psi} = c_1 \mathbf{P}_1^t : \dot{\mathbf{F}}_1 + c_2 \mathbf{P}_2^t : \dot{\mathbf{F}}_2 + \rho_2 [\psi]\dot{c}$ into the expression of dissipation Eq. (119), one obtains

$$D_V = c_1 (\mathbf{P}^t - \mathbf{P}_1^t) : \dot{\mathbf{F}}_1 + c_2 (\mathbf{P}^t - \mathbf{P}_2^t) : \dot{\mathbf{F}}_2 + X_c \dot{c} \geqslant 0, \tag{120}$$

where $X_c := \mathbf{P}^t : [\mathbf{F}] - \rho_2 [\psi]$ is the Eshelby driving force for change in volume fraction (interface propagation) during the phase transformation $1 \leftrightarrow 2$.

Now we transform the two first terms in Eq. (120). Utilizing the second Eq. (114) $\mathbf{P}^t = (1 - c)\mathbf{P}_1^t + c\mathbf{P}_2^t$, we obtain $\mathbf{P}^t - \mathbf{P}_1^t = c[\mathbf{P}^t]$ and $\mathbf{P}^t - \mathbf{P}_2^t = (c - 1)[\mathbf{P}^t]$. Then

$$c_1 (\mathbf{P}^t - \mathbf{P}_1^t) : \dot{\mathbf{F}}_1 + c_2 (\mathbf{P}^t - \mathbf{P}_2^t) : \dot{\mathbf{F}}_2 = -c_1 c_2 [\mathbf{P}^t] : (\dot{\mathbf{F}}_2 - \dot{\mathbf{F}}_2) = -c_1 c_2 [\mathbf{P}^t] : [\dot{\mathbf{F}}]$$

$$= -c_1 c_2 [\mathbf{P}] : [\dot{\mathbf{F}}^t]. \tag{121}$$

Using the Hadamard compatibility condition and the traction continuity condition

$$[\mathbf{F}] = \mathbf{a}\mathbf{n}, \quad [\mathbf{P}] \cdot \mathbf{n} = 0, \tag{122}$$

Eq. (121) can be further transformed to

$$-c_1 c_2 [\mathbf{P}] : [\dot{\mathbf{F}}^t] = -c_1 c_2 [\mathbf{P}] : (\overline{\mathbf{n}\mathbf{a}}) = -c_1 c_2 [\mathbf{P}] : (\dot{\mathbf{n}}\mathbf{a} + \mathbf{n}\dot{\mathbf{a}}) = -c_1 c_2 [\mathbf{P}] : \dot{\mathbf{n}}\mathbf{a}$$

$$= -c_1 c_2 \mathbf{a} \cdot [\mathbf{P}] \cdot \dot{\mathbf{n}}. \tag{123}$$

Consequently, the dissipation rate (120) can be presented in the form

$$D_V = X_c \dot{c} + \mathbf{X}_n \cdot \dot{\mathbf{n}} \geqslant 0, \tag{124}$$

where

$$\mathbf{X}_n := -c_1 c_2 \mathbf{a} \cdot [\mathbf{P}] \tag{125}$$

is the universal thermodynamic driving force for interface rotation.

Now we decompose $\mathbf{a} = a_n \mathbf{n} + a_\tau \boldsymbol{\tau}$, where $a_n$ and $a_\tau$ are the scalar component of the vector $\mathbf{a}$ along the normal $\mathbf{n}$ and the unit vector $\boldsymbol{\tau}$ within the interface $\Sigma$. Let us consider the coordinate system 1–2–3 with axis 1 along the $\boldsymbol{\tau}$, axis 2 along the normal $\mathbf{n}$ and axis 3 orthogonal to both of them (Fig. 2b). Since $\mathbf{P}$ is not symmetric and $\mathbf{n} \cdot [\mathbf{P}] \neq 0$, the component of the vector $\mathbf{a}$ along the normal, $a_n \mathbf{n}$, cannot be excluded as in the case of small strain (see Eq. (13)). In this local coordinate system $\boldsymbol{\tau} = (1, 0, 0)$, $\mathbf{n} = (0, 1, 0)$ and $[P_{12}] = [P_{22}] = [P_{32}] = 0$ due to traction continuity condition. Then the components of the driving force $\mathbf{X}_n$ in this coordinate system are

$$X_n^1 = -c_1 c_2 (a_\tau [P_{11}] + a_n [P_{21}]), \quad X_n^2 = -c_1 c_2 (a_\tau [P_{12}] + a_n [P_{22}]) = 0,$$
$$X_n^3 = -c_1 c_2 (a_\tau [P_{13}] + a_n [P_{23}]), \tag{126}$$

i.e. vector $\mathbf{X}_n$ belongs to the interface. The conditions for thermodynamic orientational equilibrium for the case with $k = 0$, $X_n^1 = X_n^2 = 0$, are

$$-\frac{a_\tau}{a_n} = \frac{[P_{21}]}{[P_{11}]} = \frac{[P_{23}]}{[P_{13}]}. \tag{127}$$

If $a_n = 0$, then $[P_{11}] = [P_{13}] = 0$; when $a_\tau = 0$, then $[P_{21}] = [P_{23}] = 0$.

## 7. Some relations for finite inelastic deformation of microheterogeneous materials with moving discontinuity interfaces

In this section two problems will be addressed. The first one is related to finding conditions under which our considerations in Sections 2 and 6 are justified from the point of view of the general theory of the micro- to macro transition for microheterogeneous materials with moving discontinuity surfaces. The second problem is concerned with the question of why the driving force for the interface reorientation did not follow from the general energetic consideration of the phase transformation in Eshelby (1956), Kaganova and Roitburd (1988) and Grinfeld (1991). Let us consider in a reference configuration $V_\tau$ the representative volume $\upsilon$ of an inelastic material bounded by a surface $S$ and made up by vectors $\tilde{r}_\tau$ at time $t = \tau$ (here $\sim$ means local values of parameters). The motion is described by the function $\tilde{r}(\tilde{r}_\tau, t)$, where $\tilde{r}$ is the position vector in an actual configuration $V_t$. The deformation gradient $\tilde{F} = \nabla \tilde{r}$ and the nonsymmetric Piola–Kirchhoff stress tensor $\tilde{P}$ are determined with respect to $V_\tau$. The velocity $\dot{\tilde{r}}(\tilde{r}_\tau, t)$ and deformation gradient $\tilde{F}$ undergo discontinuities on the interfaces $\Sigma$ (possibly multi-connected) moving with normal velocity $\upsilon_n$. We consider a coherent phase transformation only, for which the jump of the position vector $[\tilde{r}] = 0$ is across the interface. Due to the Hadamard compatibility condition

$$[\boldsymbol{F}_\tau] = -[\upsilon]\boldsymbol{n}_\tau/\upsilon_n, \quad \text{hence} \quad [\upsilon] = -[\boldsymbol{F}_\tau] \cdot \boldsymbol{n}_\tau \upsilon_n$$
$$\text{and} \quad [\boldsymbol{F}_\tau] = [\boldsymbol{F}_\tau] \cdot \boldsymbol{n}_\tau \boldsymbol{n}_\tau. \tag{128}$$

It follows from the equilibrium equations that across the interface

$$[\widetilde{\boldsymbol{P}}] \cdot \boldsymbol{n} = [\dot{\widetilde{\boldsymbol{P}}}] \cdot \boldsymbol{n} = 0. \tag{129}$$

The macroscopic variables for materials with the moving discontinuity surfaces of the velocity vector have been introduced in Levitas (1992, 1996b) and Petryk (1998). The energy relationships have been derived in Levitas (1992, 1996b) and Petryk (1998) for the macroscopically homogeneous boundary conditions, namely for stresses corresponding to constant stress or for displacements corresponding to the constant deformation gradient. Here we will consider two phase material with more sophisticated boundary conditions when the external surface consists of two parts (phases 1 and 2), and the macroscopically homogeneous boundary conditions at each of them correspond to two different constant stress (or deformation gradient) tensors.

### 7.1. Macroscopic variables and energy identities

The macroscopic tensors will be defined as in Hill's (1984) work

$$\boldsymbol{F} := \frac{1}{\upsilon} \int_S \tilde{r}\boldsymbol{n} \quad \mathrm{d}S, \quad \boldsymbol{P}^{\mathrm{t}} := \frac{1}{\upsilon} \int_S \tilde{r}_\tau \widetilde{\boldsymbol{P}} \cdot \boldsymbol{n} \, \mathrm{d}S. \tag{130}$$

Defining the macroscopic tensors for each phase in a similar way,

$$\boldsymbol{F}_1 := \frac{1}{\upsilon_1} \int_{S_1+\Sigma} \tilde{r}\boldsymbol{n} \, \mathrm{d}S, \quad \boldsymbol{F}_2 := \frac{1}{\upsilon_2} \int_{S_2+\Sigma} \tilde{r}\boldsymbol{n} \, \mathrm{d}S, \tag{131}$$

$$\boldsymbol{P}_1^{\mathrm{t}} := \frac{1}{\upsilon_1} \int_{S_1+\Sigma} \tilde{r}_\tau \widetilde{\boldsymbol{P}} \cdot \boldsymbol{n} \, \mathrm{d}S, \quad \boldsymbol{P}_2^{\mathrm{t}} := \frac{1}{\upsilon_2} \int_{S_2+\Sigma} \tilde{r}_\tau \widetilde{\boldsymbol{P}} \cdot \boldsymbol{n} \, \mathrm{d}S, \tag{132}$$

one can check the validity of the following equations:

$$F = c_1 F_1 + c_2 F_2, \quad P = c_1 P_1 + c_2 P_2, \quad c_1 := \frac{v_1}{v}, \quad c_2 := \frac{v_2}{v} \tag{133}$$

by direct substitution. Here $v_i$ and $c_i$ are the volume and the volume fraction of the $i$th phase in the reference configuration and the continuity of the position vector $[\tilde{r}_\tau] = 0$ and the traction vector $[\widetilde{P} \cdot n] = 0$ is taken into account.

The general scheme of the application of the Gauss theorem is the following one. The volume $v$ is divided by surfaces $\Sigma$ and $S$ into a finite number of volumes. In each of the volumes all functions are continuous and, using the Gauss theorem, we obtain some equations. After summing up all these equations we obtain an integral over the volume $\bar{v} = v - \Sigma$ at one side and on other side an integral on $S$ and integral on $\Sigma$ of the jump of functions (because the integration on $\Sigma$ is performed two times for two volumes, divided by $\Sigma$). Using the Gauss theorem we derive

$$F = \langle \widetilde{F} \rangle, \quad P^{\mathrm{t}} = \langle \widetilde{P}^{\mathrm{t}} \rangle, \tag{134}$$

$$F_i = \langle \widetilde{F} \rangle_i, \quad P_i^{\mathrm{t}} = \langle \widetilde{P}^{\mathrm{t}} \rangle_i, \tag{135}$$

where $\langle \tilde{a} \rangle := \frac{1}{v} \int \tilde{a} \, dv$ and $\langle \tilde{a} \rangle_i := \frac{1}{v_i} \int \tilde{a} \, dv_i$ designate volume average over the entire volume $v$ and the volume of each phase. Direct calculations using the Gauss theorem, definition of the macroscopic variables (Eqs. (134) and (135)) and the equilibrium equation inside the volumes $v_i$ ($\nabla \cdot \widetilde{P} = 0$) prove the identities

$$\frac{1}{v} \int_S (\tilde{r} - F \cdot \tilde{r}_\tau)(\widetilde{P} - P) \cdot n \, dS = \langle \widetilde{F} \cdot \widetilde{P}^{\mathrm{t}} \rangle - F \cdot P^{\mathrm{t}}, \tag{136}$$

$$\frac{1}{v_i} \int_{S_i + \Sigma} (\tilde{r} - F_i \cdot \tilde{r}_\tau)(\widetilde{P} - P_i) \cdot n \, dS = \langle \widetilde{F} \cdot \widetilde{P}^{\mathrm{t}} \rangle_i - F_i \cdot P_i^{\mathrm{t}}. \tag{137}$$

Due to the continuity of the position vector $[\tilde{r}_\tau] = 0$ and the traction vector $[\widetilde{P} \cdot n] = 0$ across the interface, these equations coincide with those for the representative volume without the discontinuity surfaces. The energetic equality

$$\langle \widetilde{F} \cdot \widetilde{P}^{\mathrm{t}} \rangle = F \cdot P^{\mathrm{t}} \tag{138}$$

is valid when the surface integral in Eq. (136) is zero. This is true, in particular, for the macroscopically homogeneous boundary conditions at the external surface $S$: $\tilde{r} = F_0 \cdot \tilde{r}_\tau$ or $\widetilde{P} \cdot n = P_0 \cdot n$, where $F_0$ and $P_0$ are some constant tensors. For such boundary conditions, Eqs. (130) results in $F = F_0$ or $P = P_0$. Eq. (138) is also valid when $\tilde{r} = F_0 \cdot \tilde{r}_\tau$ at one part of the external surface $S$ and $\widetilde{P} \cdot n = P_0 \cdot n$ at another one. However, we cannot prove that $F = F_0$ or $P = P_0$ in this case. In a similar way, the energetic equality for each phase

$$\langle \widetilde{F} \cdot \widetilde{P}^{\mathrm{t}} \rangle_i = F_i \cdot P_i^{\mathrm{t}} \tag{139}$$

is valid when the surface integral in Eq. (137) is zero. This is true, in particular, for the macroscopically homogeneous boundary conditions at the surface $S_i + \Sigma$: $\tilde{r} = F_{0i} \cdot \tilde{r}_\tau$ or $\widetilde{P} \cdot n = P_{0i} \cdot n$, where $F_{0i}$ and $P_{0i}$ are some constant tensors. For such boundary conditions, Eqs. (131) and (132) result in $F_i = F_{0i}$ or $P_i = P_{0i}$. However, since $\Sigma$ is the internal surface, stresses and displacements at it cannot be prescribed but rather determined from the solution of the boundary-value problem. That is why the above conditions and Eq. (139) are valid for the very special interfaces, otherwise their use is quite a strong simplifying assumption.

### 7.2. Macroscopically piece-wise homogeneous boundary conditions

Let the external surface $S$ consists of two parts $S_1$ and $S_2$ that belong to phases 1 and 2. We prescribe macroscopically homogeneous boundary conditions on the surfaces $S_1$ and $S_2$, respectively:

$$\text{at } S_1 : \quad \tilde{r} = F_{10} \cdot \tilde{r}_\tau \quad \text{or} \quad \widetilde{P} \cdot n = P_{10} \cdot n, \tag{140}$$

$$\text{at } S_2 : \quad \tilde{r} = F_{20} \cdot \tilde{r}_\tau \quad \text{or} \quad \widetilde{P} \cdot n = P_{20} \cdot n. \tag{141}$$

First we will find at which conditions at the interface $\Sigma$, tensors $F_{i0}$ and $P_{i0}$ represent the macroscopic deformation gradient and stress in each phase. One gets

$$F_i := \frac{1}{v_i} \int_{S_i} F_{i0} \cdot \tilde{r}_\tau n_i \, \mathrm{d}S + \frac{1}{v_i} \int_\Sigma \tilde{r} n_i \, \mathrm{d}S = \frac{1}{v_i} \int_{S_i+\Sigma} F_{i0} \cdot \tilde{r}_\tau n_i \, \mathrm{d}S + \frac{1}{v_i} \int_\Sigma (\tilde{r} - F_{i0} \cdot \tilde{r}_\tau) n_i \, \mathrm{d}\Sigma = F_{i0} \tag{142}$$

$$+ \frac{1}{v_i} \int_\Sigma (\tilde{r} - F_{i0} \cdot \tilde{r}_\tau) n_i \, \mathrm{d}\Sigma P_i^t = \frac{1}{v_i} \int_{S_i} \tilde{r}_\tau P_{i0} \cdot n_i \, \mathrm{d}S + \frac{1}{v_i} \int_\Sigma \tilde{r}_\tau \widetilde{P} \cdot n_i \, \mathrm{d}\Sigma$$

$$= \frac{1}{v_i} \int_{S_i+\Sigma} \tilde{r}_\tau P_{i0} \cdot n_i \, \mathrm{d}S + \frac{1}{v_i} \int_\Sigma \tilde{r}_\tau (\widetilde{P} - P_{i0}) \cdot n_i \, \mathrm{d}\Sigma = P_{i0}^t + + \frac{1}{v_i} \int_\Sigma \tilde{r}_\tau (\widetilde{P} - P_{i0}) \cdot n_i \, \mathrm{d}\Sigma \tag{143}$$

It is clear that necessary and sufficient conditions for the equalities $F_i = F_{i0}$ and $P_i = P_{i0}$ are

$$\int_\Sigma (\tilde{r} - F_{i0} \cdot \tilde{r}_\tau) n_i \, \mathrm{d}\Sigma = 0 \quad \text{and} \quad \int_\Sigma \tilde{r}_\tau (\widetilde{P} - P_{i0}) \cdot n_i \, \mathrm{d}\Sigma = 0, \tag{144}$$

respectively. These conditions are weaker than the requirement of macroscopically homogeneous boundary data, because they prescribe the same constraint averaged over the interface rather than point-wise. If one of Eqs. (144) is valid, then from Eqs. (133) one of the following equations yields

$$F = c_1 F_{10} + c_2 F_{20} \quad \text{or} \quad P = c_1 P_{10} + c_2 P_{20}. \tag{145}$$

Substituting macroscopically piece-wise homogeneous boundary conditions Eqs. (140) and (141) either for the position vector or for the stress tensor in the left hand side of Eq. (137) under fulfillment of one of Eqs. (144), one obtains for the left-hand side of Eq. (137)

$$\int_{S_i+\Sigma} (\tilde{r} - F_{i0} \cdot \tilde{r}_\tau)(\widetilde{P} - P_i) \cdot n_i \, \mathrm{d}S = \int_\Sigma (\tilde{r} - F_{i0} \cdot \tilde{r}_\tau)(\widetilde{P} - P_i) \cdot n_i \, \mathrm{d}S$$

$$= \int_\Sigma (\tilde{r} - F_{i0} \cdot \tilde{r}_\tau)\widetilde{P} \cdot n_i \, \mathrm{d}S - \int_\Sigma (\tilde{r} - F_{i0} \cdot \tilde{r}_\tau) n_i \, \mathrm{d}S \cdot P^t = \int_\Sigma (\tilde{r} - F_{i0} \cdot \tilde{r}_\tau)\widetilde{P} \cdot n_i \, \mathrm{d}S, \tag{146}$$

$$\int_{S_i+\Sigma} (\tilde{r} - F_i \cdot \tilde{r}_\tau)(\widetilde{P} - P_{0i}) \cdot n_i \, \mathrm{d}S = \int_\Sigma (\tilde{r} - F_i \cdot \tilde{r}_\tau)(\widetilde{P} - P_{0i}) \cdot n_i \, \mathrm{d}S$$

$$= \int_\Sigma \tilde{r}(\widetilde{P} - P_{0i}) \cdot n_i \, \mathrm{d}S - F_i \cdot \int_\Sigma \tilde{r}_\tau (\widetilde{P} - P_{0i}) \cdot n_i \, \mathrm{d}S = \int_\Sigma \tilde{r}(\widetilde{P} - P_{0i}) \cdot n_i \, \mathrm{d}S. \tag{147}$$

We have to require one of the conditions

$$\int_{\Sigma} (\tilde{r} - F_{i0} \cdot \tilde{r}_\tau)\widetilde{P} \cdot n_i \, dS = 0 \qquad \text{or} \qquad \int_{\Sigma} \tilde{r}(\widetilde{P} - P_{0i}) \cdot n_i \, dS = 0 \tag{148}$$

in order to have the desirable identities of Eq. (139). The first of these conditions, Eq. $(148)_1$ is satisfied exactly, if on $\Sigma$ we prescribe the same Eqs. (140) and $(141)_1$ for $\tilde{r}$ as on $S_i$. The second condition Eq. $(148)_2$ is satisfied exactly, if on $\Sigma$ we prescribe the same Eqs. (140) and $(141)_2$ for $\widetilde{P} \cdot n_i$ as on $S_i$. However, conditions Eq. (148) are weaker, as they require the integrals over the interface to be zero rather than local parameters in each point of the interface. When Eq. (148) are valid, then

$$\langle \widetilde{F} \cdot \widetilde{P}^{\mathrm{t}} \rangle = c_1 \langle \widetilde{F} \cdot \widetilde{P}^{\mathrm{t}} \rangle_1 + c_2 \langle \widetilde{F} \cdot \widetilde{P}^{\mathrm{t}} \rangle_2 = c_1 F_1 \cdot P_1^{\mathrm{t}} + c_2 F_2 \cdot P_2^{\mathrm{t}}. \tag{149}$$

Let us now find under which additional conditions the equation for the entire volume

$$\langle \widetilde{F} \cdot \widetilde{P}^{\mathrm{t}} \rangle = F \cdot P^{\mathrm{t}} \tag{150}$$

is valid as well. The derivation is a little bit bulky. First, let us calculate the left-hand side of Eq. (136) for the macroscopically piece-wise homogeneous boundary data in the position vector Eq. $(140)_1$ and $(141)_1$. We have

$$
\begin{aligned}
\int_S (\tilde{r} - F \cdot \tilde{r}_\tau)(\widetilde{P} - P) \cdot n \, dS &= \int_{S_1} (F_{01}\tilde{r}_\tau - F \cdot \tilde{r}_\tau)(\widetilde{P} - P) \cdot n_1 \, dS \\
&\quad + \int_{S_2} (F_{02}\tilde{r}_\tau - F \cdot \tilde{r}_\tau)(\widetilde{P} - P) \cdot n_2 \, dS = (F_{01} - F) \\
&\quad \cdot \int_{S_1} \tilde{r}_\tau(\widetilde{P} - P) \cdot n_1 \, dS + (F_{02} - F) \cdot \int_{S_2} \tilde{r}_\tau(\widetilde{P} - P) \cdot n_2 \, dS \\
&= (F_{01} - F) \cdot \int_{S_1 + \Sigma} \tilde{r}_\tau(\widetilde{P} - P) \cdot n_1 \, dS + (F_{02} - F) \\
&\quad \cdot \int_{S_2 + \Sigma} \tilde{r}_\tau(\widetilde{P} - P) \cdot n_2 \, dS - (F_{01} - F) \\
&\quad \cdot \int_\Sigma \tilde{r}_\tau(\widetilde{P} - P) \cdot n_1 \, dS - (F_{02} - F) \cdot \int_\Sigma \tilde{r}_\tau(\widetilde{P} - P) \cdot n_2 \, dS \\
&= (F_{01} - F) \cdot (P_1^{\mathrm{t}} - P^{\mathrm{t}})v_1 + (F_{02} - F) \cdot (P_2^{\mathrm{t}} - P^{\mathrm{t}})v_2 \\
&\quad + (F_{02} - F_{01}) \cdot \int_\Sigma \tilde{r}_\tau(\widetilde{P} - P) \cdot n_1 \, dS = v_1 F_{01} \cdot P_1^{\mathrm{t}} \\
&\quad + v_2 F_{02} \cdot P_2^{\mathrm{t}} - v F \cdot P^{\mathrm{t}} + (F_{02} - F_{01}) \cdot \int_\Sigma \tilde{r}_\tau(\widetilde{P} - P) \cdot n_1 \, dS.
\end{aligned}
\tag{151}
$$

The substitution of this result into Eq. (136) with allowing for Eq. (149) yields the important equality

$$(F_{02} - F_{01}) \cdot \int_\Sigma \tilde{r}_\tau(\widetilde{P} - P) \cdot n_i \, dS = 0. \tag{152}$$

Let us now again calculate the left-hand side of Eq. (136) using the other way

$$\int_S (\tilde{\boldsymbol{r}} - \boldsymbol{F} \cdot \tilde{\boldsymbol{r}}_\tau)(\widetilde{\boldsymbol{P}} - \boldsymbol{P}) \cdot \boldsymbol{n}\,\mathrm{d}S = (\boldsymbol{F}_{01} - \boldsymbol{F}) \cdot \int_{S_1} \tilde{\boldsymbol{r}}_\tau(\widetilde{\boldsymbol{P}} - \boldsymbol{P}) \cdot \boldsymbol{n}_1\,\mathrm{d}S$$

$$+ (\boldsymbol{F}_{02} - \boldsymbol{F}) \cdot \int_{S_2} \tilde{\boldsymbol{r}}_\tau(\widetilde{\boldsymbol{P}} - \boldsymbol{P}) \cdot \boldsymbol{n}_2\,\mathrm{d}S$$

$$= (\boldsymbol{F}_{01} - \boldsymbol{F}) \cdot \int_S \tilde{\boldsymbol{r}}_\tau(\widetilde{\boldsymbol{P}} - \boldsymbol{P}) \cdot \boldsymbol{n}\,\mathrm{d}S + (\boldsymbol{F}_{02} - \boldsymbol{F}_{01})$$

$$\cdot \int_{S_2} \tilde{\boldsymbol{r}}_\tau(\widetilde{\boldsymbol{P}} - \boldsymbol{P}) \cdot \boldsymbol{n}_2\,\mathrm{d}S = (\boldsymbol{F}_{02} - \boldsymbol{F}_{01}) \cdot \int_{S_2} \tilde{\boldsymbol{r}}_\tau(\widetilde{\boldsymbol{P}} - \boldsymbol{P}) \cdot \boldsymbol{n}_2\,\mathrm{d}S$$

$$= (\boldsymbol{F}_{02} - \boldsymbol{F}_{01}) \cdot \int_{S_2+\Sigma} \tilde{\boldsymbol{r}}_\tau(\widetilde{\boldsymbol{P}} - \boldsymbol{P}) \cdot \boldsymbol{n}_2\,\mathrm{d}S$$

$$= (\boldsymbol{F}_{02} - \boldsymbol{F}_{01}) \cdot (\boldsymbol{P}_2^{\mathrm{t}} - \boldsymbol{P}^{\mathrm{t}})v_2. \tag{153}$$

We added to the first term and subtracted from the second term of the first line of Eq. (152) the integral $(\boldsymbol{F}_{01} - \boldsymbol{F}) \cdot \int_{S_2} \tilde{\boldsymbol{r}}_\tau(\widetilde{\boldsymbol{P}} - \boldsymbol{P}) \cdot \boldsymbol{n}_2\,\mathrm{d}S$ and then used the definition in Eq. (130) of the macroscopic stress, and finally, Eq. (152). Using Eq. (145), one obtains $\boldsymbol{P}_2^{\mathrm{t}} - \boldsymbol{P}^{\mathrm{t}} = c_1(\boldsymbol{P}_2^{\mathrm{t}} - \boldsymbol{P}_1^{\mathrm{t}})$. Thus,

$$\frac{1}{v}\int_S (\tilde{\boldsymbol{r}} - \boldsymbol{F} \cdot \tilde{\boldsymbol{r}}_\tau)(\widetilde{\boldsymbol{P}} - \boldsymbol{P}) \cdot \boldsymbol{n}\,\mathrm{d}S = c_1 c_2 (\boldsymbol{F}_{01} - \boldsymbol{F}_{02}) \cdot (\boldsymbol{P}_2^{\mathrm{t}} - \boldsymbol{P}_1^{\mathrm{t}}). \tag{154}$$

Consequently, Eq. (150) is valid at

$$(\boldsymbol{F}_{01} - \boldsymbol{F}_{02}) \cdot (\boldsymbol{P}_2^{\mathrm{t}} - \boldsymbol{P}_1^{\mathrm{t}}) = 0. \tag{155}$$

For macroscopically homogeneous boundary conditions at the entire surface $S$ one has either $\boldsymbol{F}_{02} = \boldsymbol{F}_{01}$ or $\boldsymbol{P}_1 = \boldsymbol{P}_2 = \boldsymbol{P}$, so these conditions are fulfilled automatically. Otherwise, conditions Eq. (155) are quite restrictive. However, for the following particular case they can be made much weaker. Assume a plane interface $\Sigma$ and that the difference $\boldsymbol{F}_{02} - \boldsymbol{F}_{01}$ satisfies the condition

$$\boldsymbol{F}_{02} - \boldsymbol{F}_{01} = (\boldsymbol{F}_{02} - \boldsymbol{F}_{01}) \cdot \boldsymbol{n}\boldsymbol{n}, \tag{156}$$

the same as for the jump in the deformation gradient across the interface at each point of interface, see Eq. (128). Then from Eq. (155) one obtains

$$(\boldsymbol{F}_{01} - \boldsymbol{F}_{02}) \cdot (\boldsymbol{P}_2^{\mathrm{t}} - \boldsymbol{P}_1^{\mathrm{t}}) = (\boldsymbol{F}_{02} - \boldsymbol{F}_{01}) \cdot \boldsymbol{n}\boldsymbol{n} \cdot (\boldsymbol{P}_2^{\mathrm{t}} - \boldsymbol{P}_1^{\mathrm{t}}) = 0. \tag{157}$$

Eq. (157) can be met at

$$\boldsymbol{P}_1 \cdot \boldsymbol{n} = \boldsymbol{P}_2 \cdot \boldsymbol{n}, \tag{158}$$

i.e. only tractions at the interface corresponding to $\boldsymbol{P}_1$ and $\boldsymbol{P}_2$ have to be the same (similar to the traction continuity condition across the interface at each point of interface).

For the macroscopically piece-wise homogeneous boundary conditions for the traction vector Eqs. $(140)_2$ and $(141)_2$, in a similar way one derives the identity

$$\int_\Sigma (\tilde{\boldsymbol{r}} - \boldsymbol{F} \cdot \tilde{\boldsymbol{r}}_\tau)\boldsymbol{n}\,\mathrm{d}S \cdot (\boldsymbol{P}_{02}^{\mathrm{t}} - \boldsymbol{P}_{01}^{\mathrm{t}}) = 0 \tag{159}$$

and calculates

$$\frac{1}{v}\int_S (\tilde{\boldsymbol{r}} - \boldsymbol{F} \cdot \tilde{\boldsymbol{r}}_\tau)(\widetilde{\boldsymbol{P}} - \boldsymbol{P}) \cdot \boldsymbol{n}\,\mathrm{d}S = c_1 c_2 (\boldsymbol{F}_1 - \boldsymbol{F}_2) \cdot (\boldsymbol{P}_{02}^{\mathrm{t}} - \boldsymbol{P}_{01}^{\mathrm{t}}). \tag{160}$$

Consequently, Eq. (150) is valid at

$$(F_1 - F_2) \cdot (P_{02}^t - P_{01}^t) = 0. \tag{161}$$

This condition is similar to Eq. (155) and derivations similar to those in Eqs. (156)–(158) can be performed.

Summarizing, for macroscopically piece-wise homogeneous boundary conditions on the surfaces $S_1$ and $S_2$ (Eqs. (140) and (141)), equalities for each phase $F_i = F_{i0}$ and $P_i = P_{i0}$ and Eqs. $(145)_1$ and $(145)_2$ are valid under conditions Eqs. $(144)_1$ and $(144)_2$, respectively; Eqs. (139) and (149) are true under additional constrain Eq. (148). For the entire volume, Eq. (150) is valid under additional constraint Eq. (155) for prescribed position vectors or at Eq. (161) for prescribed tractions. These constrains can be met for plane interface and conditions Eqs. (156) and (158) that are similar to the local Hadamard compatibility and traction continuity conditions. The main result is that if we assume the homogeneous deformation gradients and stresses in each phase and plane interface (or multiple plain parallel interfaces), then all constrains are met and Eqs. (139) and (150) are valid. Also, Eqs. (136)–(139), (146)–(155), (157) and (159)–(161) are tensorial equations. In applications, one needs scalar energetic relationships, which can be obtained by calculating the trace of all the above mentioned equations. For example, instead of Eqs. (153) and (150) one obtains

$$\int_S (\tilde{r} - F \cdot \tilde{r}_\tau) \cdot (\widetilde{P} - P) \cdot n \, \mathrm{d}S = (F_{02} - F_{01}) : (P_2^t - P^t) v_2, \tag{162}$$

$$\langle \widetilde{F} : \widetilde{P}^t \rangle = F : P^t. \tag{163}$$

### 7.3. Macroscopic rate of deformation gradient and stress power

Let us define the rate of the macroscopic deformation gradient and stress tensor by differentiating Eq. (130):

$$\dot{F} := \frac{1}{v} \int_S \dot{\tilde{r}} n \, \mathrm{d}S = \langle \dot{\widetilde{F}} \rangle + \frac{1}{v} \int_\Sigma [\widetilde{F}] v_n \, \mathrm{d}\Sigma. \tag{164}$$

For plane interface and homogeneous parameters in each phase, Eq. (164) transforms to

$$\dot{F} = c_1 \dot{F}_1 + c_2 \dot{F}_2 + [F] \dot{c}, \tag{165}$$

since $v_n \Sigma / v = \dot{c}$. Eq. (165) coincides with the result of direct differentiation of Eq. (133) and it is independent of boundary conditions. Now we have to find conditions under which the power of external stresses can be presented in the form

$$\frac{1}{v} \int \dot{\tilde{r}} \cdot \widetilde{P} \cdot n \, \mathrm{d}S = \dot{F} : P^t \tag{166}$$

that was used in Eq. (119). Direct calculations using the Gauss theorem results in the equality

$$\frac{1}{v} \int_\Sigma (\dot{\tilde{r}} - \dot{F} \cdot \tilde{r}_\tau)(\widetilde{P} - P) \cdot n \, \mathrm{d}S = \langle \dot{\widetilde{F}} \cdot \widetilde{P}^t \rangle - \dot{F} \cdot P^t + \frac{1}{v} \int_\Sigma [\widetilde{F}] \cdot \widetilde{P}^t v_n \, \mathrm{d}\Sigma. \tag{167}$$

Indeed,

$$\frac{1}{\upsilon}\int(\dot{\tilde{r}} - \dot{F}\cdot\tilde{r}_\tau)(\widetilde{P} - P)\cdot n\,\mathrm{d}S = \langle(\dot{\widetilde{F}} - \dot{F})\cdot(\widetilde{P}^\mathrm{t} - P^\mathrm{t})\rangle - \frac{1}{\upsilon}\int_\Sigma([\dot{\tilde{r}}\widetilde{P}]\cdot n - [\dot{\tilde{r}}]n\cdot P^\mathrm{t})\,\mathrm{d}\Sigma$$

$$= \langle\dot{\widetilde{F}}\cdot\widetilde{P}^\mathrm{t}\rangle + (\dot{F}\cdot P^\mathrm{t} - \dot{F}\cdot\langle\widetilde{P}^\mathrm{t}\rangle) - (\langle\dot{\widetilde{F}}\rangle\cdot P^\mathrm{t}$$

$$+ \frac{1}{\upsilon}\int_\Sigma[\widetilde{F}]v_n\,\mathrm{d}\Sigma\cdot P^\mathrm{t}) + \frac{1}{\upsilon}\int_\Sigma[\widetilde{F}]\cdot\widetilde{P}^\mathrm{t}v_n\,\mathrm{d}\Sigma. \qquad (168)$$

We used $[\dot{\tilde{r}}\widetilde{P}]\cdot n = [\dot{\tilde{r}}]\widetilde{P}\cdot n = [\dot{\tilde{r}}]n\cdot\widetilde{P}^\mathrm{t}$ due to traction continuity condition across the interface and $[\dot{\tilde{r}}]n = -[F]v_n$ due to the Hadamard compatibility condition (see Eq. (128)). The term in the first parenthesis is zero because of $P^\mathrm{t} = \langle\widetilde{P}^\mathrm{t}\rangle$. The second parenthesis can be transformed to $\dot{F}\cdot P^\mathrm{t}$ because of the expression for $\dot{F}$ in Eq. (164), thus completing the proof of Eq. (167).

Using similar calculations, we obtain

$$\frac{1}{\upsilon}\int_\Sigma\dot{\tilde{r}}\widetilde{P}\cdot n\,\mathrm{d}S = \langle\dot{\widetilde{F}}\cdot\widetilde{P}^\mathrm{t}\rangle + \frac{1}{\upsilon}\int_\Sigma[\widetilde{F}]\cdot\widetilde{P}^\mathrm{t}v_n\,\mathrm{d}\Sigma. \qquad (169)$$

Combining Eqs. (167) and (169), we find

$$\frac{1}{\upsilon}\int_\Sigma\dot{\tilde{r}}\widetilde{P}\cdot n\,\mathrm{d}S = \frac{1}{\upsilon}\int_\Sigma(\dot{\tilde{r}} - \dot{F}\cdot\tilde{r}_\tau)(\widetilde{P} - P)\cdot n\,\mathrm{d}S + \dot{F}\cdot P^\mathrm{t}. \qquad (170)$$

### 7.3.1. Macroscopically homogeneous boundary conditions

For macroscopically homogeneous boundary conditions at the entire external surface for the velocity or traction vectors ($\dot{\tilde{r}} = \dot{F}\cdot\tilde{r}_\tau$ or $\widetilde{P}\cdot n = P\cdot n$), the left hand side of Eq. (167) tends to zero and one obtains

$$\dot{F} : P^\mathrm{t} = \langle\dot{\widetilde{F}} : \widetilde{P}^\mathrm{t}\rangle_\tau + \frac{1}{\upsilon}\int_\Sigma[\widetilde{F}] : \widetilde{P}^\mathrm{t}v_n\,\mathrm{d}\Sigma. \qquad (171)$$

Combining Eqs. (169) and (171) we derive

$$\frac{1}{\upsilon}\int\dot{\tilde{r}}\widetilde{P}\cdot n\,\mathrm{d}S = \dot{F}\cdot P^\mathrm{t}. \qquad (172)$$

Calculating the trace of Eq. (172), we complete the proof of Eq. (166). Thus, for the macroscopically homogeneous boundary conditions expression for stress power that we used in Eq. (119) is correct.

### 7.3.2. Macroscopically piece-wise homogeneous boundary conditions

Let us derive the expression for the stress power for the piece-wise homogeneous boundary conditions Eqs. (140) and (141). We will start with transformations similar to ones in Eq. (151):

$$\int_S(\dot{\tilde{r}} - \dot{F}\cdot\tilde{r}_\tau)(\widetilde{P} - P)\cdot n\,\mathrm{d}S = \int_{S_1}(\dot{F}_{01}\tilde{r}_\tau - \dot{F}\cdot\tilde{r}_\tau)(\widetilde{P} - P)\cdot n_1\,\mathrm{d}S$$

$$+ \int_{S_2}(\dot{F}_{02}\tilde{r}_\tau - \dot{F}\cdot\tilde{r}_\tau)(\widetilde{P} - P)\cdot n_2\,\mathrm{d}S = (\dot{F}_{01} - \dot{F})$$

$$
\cdot \int_{S_1} \tilde{r}_\tau(\widetilde{P} - P) \cdot n_1 \, dS + (\dot{F}_{02} - \dot{F}) \cdot \int_{S_2} \tilde{r}_\tau(\widetilde{P} - P) \cdot n_2 \, dS
$$

$$
= (F_{01} - F) \cdot \int_{S_1+\Sigma} \tilde{r}_\tau(\widetilde{P} - P) \cdot n_1 \, dS + (F_{02} - F)
$$

$$
\cdot \int_{S_2+\Sigma} \tilde{r}_\tau(\widetilde{P} - P) \cdot n_2 \, dS - (\dot{F}_{01} - \dot{F})
$$

$$
\cdot \int_\Sigma \tilde{r}_\tau(\widetilde{P} - P) \cdot n_1 \, dS - (\dot{F}_{02} - \dot{F}) \cdot \int_\Sigma \tilde{r}_\tau(\widetilde{P} - P) \cdot n_2 \, dS
$$

$$
= (\dot{F}_{01} - \dot{F}) \cdot (P_1^t - P^t)v_1 + (\dot{F}_{02} - \dot{F}) \cdot (P_2^t - P^t)v_2
$$

$$
+ (\dot{F}_{02} - \dot{F}_{01}) \cdot \int_\Sigma \tilde{r}_\tau(\widetilde{P} - P) \cdot n_1 \, dS = c_1 c_2 v [P^t] \cdot [\dot{F}]
$$

$$
+ (\dot{F}_{02} - \dot{F}_{01}) \cdot \int_\Sigma \tilde{r}_\tau(\widetilde{P} - P) \cdot n_1 \, dS. \tag{173}
$$

The transformations in the last line are similar to those in Eq. (121). Now we assume the homogeneous deformation gradients and stresses in phases and plane interface (or plane parallel interfaces) between phase. Then the last term in Eq. (173) disappears due to the traction continuity condition and one obtains

$$
\frac{1}{v} \int_S (\dot{\tilde{r}} - \dot{F} \cdot \tilde{r}_\tau)(\widetilde{P} - P) \cdot n \, dS = c_1 c_2 [P^t] \cdot [\dot{F}]. \tag{174}
$$

Substituting Eq. (174) into Eq. (170), we have

$$
\frac{1}{v} \int_\Sigma \dot{\tilde{r}} \widetilde{P} \cdot n \, dS = c_1 c_2 [P^t] \cdot [\dot{F}] + P^t \cdot \dot{F}. \tag{175}
$$

Calculating the trace of Eq. (175) we finally obtain the expression for the power of the external stresses

$$
\frac{1}{v} \int_\Sigma \dot{\tilde{r}} \cdot \widetilde{P} \cdot n \, dS = c_1 c_2 [P^t] : [\dot{F}] + P^t : \dot{F} = -X_n \cdot \dot{n} + P^t : \dot{F}, \tag{176}
$$

where Eqs. (123) and (125) have been used.

Thus, an extra term appears in the stress power in comparison with the traditional expression Eq. (166). This term has to be added into the expression for dissipation rate Eq. (119)

$$
D_V = P^t : \dot{F} - X_n \cdot \dot{n} - \rho \dot{\psi} \geqslant 0. \tag{177}
$$

It eliminates the dissipation due to interface reorientation (see Eq. (124)) and we obtain $D_V = X_c \dot{c}$.

In summary, the thermodynamic driving force for the interface reorientation appears when macroscopically homogeneous boundary conditions in tractions or position vectors are prescribed at the entire interface, i.e. macroscopic stress or deformation gradient tensors are prescribed. Then the interface reorientation represents an additional degree of freedom and thermodynamically conjugate driving force appears in the expression for the dissipation rate. These conditions correspond to actual loading of a sample in experiments on tension–compression, torsion, biaxial loading and their combinations. On the other hands, there is no thermodynamic driving force for the interface reorientation for

macroscopically piece-wise homogeneous boundary conditions at two (several) different parts of the external surface. This explains why the driving force for reorientation did not appear in all known treatments of phase transformations leading to the expression for the local dissipation rate at each point of the interface in (Eshelby, 1956; Kaganova and Roitburd, 1988; Grinfeld, 1991): it is expressed in terms of stresses and strains from both sides of the interface (which is similar to the prescription of piece-wise boundary conditions in the current consideration) rather than some stresses or deformation gradient prescribed to some volume under study.

We analyzed macroscopically piece-wise homogeneous boundary conditions because they are consistent with the homogeneous stresses and deformation gradient in each phase. However, they do not correspond to experimental loading conditions: in all known cases macroscopically homogeneous boundary conditions are prescribed (see e.g. Abeyaratne et al., 1996). Macroscopically homogeneous boundary conditions are satisfied in an averaged sense, i.e. for tensors $F = c_1F_1 + c_2F_2$ and $P = c_1P_1 + c_2P_2$ (Ball and James, 1987; Bhattacharya, 2004; Abeyaratne et al., 1996). In this case, Eq. (166) and, consequently our expression Eq. (125) for the driving force for the interface reorientation $X_n$ is valid. In particular, they are valid for fine mixture of martensitic variants. The smaller the number of laminates is and the larger their relative size is with respect to the size of the representative volume, the larger error in the assumption of homogeneous stress–strain state of each phase because of the effect of the macroscopically homogeneous boundary conditions. Still, we can approximately apply our approach in Sections 2 and 5 even to the worst case of the representative volume having a single plain interface between phases, assuming that the inhomogeneity of strains and stresses in phases are localized near the boundary. Also, in the framework of our approach, when we use $F = c_1F_1 + c_2F_2$ and $P = c_1P_1 + c_2P_2$ instead of boundary conditions, geometric configurations in Fig. 1a and c (without martensitic variants) are equivalent provided that the volume fraction $c$ and normal $n$ are the same.

## 8. Concluding remarks

The main result of this paper is an explicit expression for the universal (i.e. independent of specific constitutive relations) thermodynamic driving force for interface reorientation, both for small and finite strains. Since we failed to find references on published papers where such a problem was formulated, an existence of such a universal driving force was not expected. It is surprisingly simple and allows us to analyze what parameters drive the interface reorientation and determine an orientational interface equilibrium without knowledge of the elastic energy. This is important because an explicit expression for energy cannot be obtained in a closed form for complex cases (for example, nonlinear elastic phases, finite strains), or else it is difficult to analyze and differentiate with respect to interface normal for anisotropic linear elastic phases under complex loading. The main reason why such a force was not revealed before is related to the fact that in the general study of the interface equilibrium and motion (Eshelby, 1956; Kaganova and Roitburd, 1988; Grinfeld, 1991), the driving force for the interface motion was derived for each interface point independent of prescribed boundary conditions. It was determined in terms of parameters from both sides of an interface, and in this case (as was shown in Section 6) the driving force for an interface reorientation does not appear. Only in the case when the macroscopically homogeneous stresses or strains are prescribed, the driving force for the interface reorientation can be found.

Another important result is related to the derivation of an explicit expression for the dissipation rate for simultaneous interface rotation and propagation for both athermal and drag interface friction and for single and multiple interfaces.

Explicit expressions for the driving forces for interface propagation and rotation versus rates of interface propagation and rotation have been derived using the extremum principles of irreversible thermodynamics. They were explicitly inversed in the form of kinetic equations for the interface propagation and rotation. An athermal friction has been taken into account for the first time while considering an interface reorientation which is very important for the realistic description of solid–solid transformations, especially for modeling metastable microstructures. An athermal friction introduces a nontrivial effect in interface motion. Because numerical implementation of obtained equations for multi-interface case requires a lot of logical operations, a simple and accurate single-function approximation of these equations was suggested. In contrast to known approaches that consider equilibrium and quasi-equilibrium microstructure in micro to macro transition, our starting point is the kinetics of a single interface, since it can be measured experimentally (Grujicic et al., 1985). Viscous interface dissipation has not been taken into account in micro to macro transition in previous papers. We found that it introduces size dependence in kinetic equations for the rate of volume fraction.

This result has an important implication in experimental determination and mathematical formulation of the kinetic equations for the rate of volume fraction that has to be studied in more detail. The above results have been used to formulate a complete system of equations for stress-induced evolution of laminated austenite–martensite microstructure, including evolution of alternating martensite I-martensite II variants within martensitic units. This evolution is coupled to the change in stress–strain state of each phase.

In Part II of our paper (Levitas and Ozsoy, 2008), the developed theory will be applied to study nontrivial stress-induced microstructure evolution for cubic-tetragonal and tetragonal-orthorhombic transformations. In future work, the expression for the athermal dissipation rate has to be generalized for the general three-dimensional orientation of the interface normal. It is not related to basic difficulties but relations may be quite bulky. Also, the entire theory has to be generalized to take into account the plastic accommodation by slip. This is a very basic and complex problem, since description of the interface propagation in plastic materials is conceptually more sophisticated than in elastic materials (Levitas, 1998, 2000).

The equations obtained here can be used as constitutive equations for finite element modeling of discrete microstructure formation in a macroscopic sample. They are much more accurate than those used in Levitas et al. (2004) and Idesman et al. (2005) for the same purposes.

## Acknowledgement

## References

Abeyaratne, R., Knowles, J.K., 1993. A continuum model of a thermoelastic solid capable of undergoing phase-transitions. J. Mech. Phys. Solids 41, 541–571.

Abeyaratne, R., Chu, C., James, R.D., 1996. Kinetics of materials with wiggly energies: theory and application to the evolution of twinning microstructures in a Cu–Al–Ni shape memory alloy. Philos. Mag. A 73, 457–497.

Artemev, A., Wang, Y., Khachaturyan, A., 2000. Three-dimensional phase field model and simulation of martensitic transformation in multilayer systems under applied stresses. Acta Mater. 48 (10), 2503–2518.

Artemev, A., Jin, Y., Khachaturyan, A., 2001. Three-dimensional phase field model of proper martensitic transformation. Acta Mater. 49 (7), 1165–1177.

Auricchio, F., Reali, A., Stefanelli, U., 2007. A three-dimensional model describing stress-induced solid phase transformation with permanent inelasticity. Int. J. Plasticity 23 (2), 207–226.

Ball, J.M., James, R.D., 1987. Fine phase mixtures as minimizers of energy. Arch. Rat. Mech. Anal. 100, 13–52.

Bhattacharya, K., 2004. Microstructure of Martensite. Why It Forms and How It Gives Rise to the Shape-Memory Effect. Oxford University Press, New York.

Chen, L.Q., 2002. Phase-Field Models for Microstructure Evolution. Annu. Rev. Mater. Res. 32, 113–140.

Eshelby, J.D., 1956. The continuum theory of lattice defects. Solid State Phys. 3, 79–144.

Eshelby, J.D., 1970. Energy relations and the energy-momentum tensor in continuum mechanics. In: Kanninen, M.F. (Ed.), Inelastic Behaviour of Solids. McGraw Hill, New York, pp. 77–115.

Gao, X., Huang, M., Brinson, L.C., 2000. A multivariant micromechanical model for SMAs. Part 1. Crystallographic issues for single crystal model. Int. J. Plasticity 16 (10), 1345–1369.

Grinfeld, M.A., 1991. Thermodynamic Methods in the Theory of Heterogeneous Systems. Longman, London.

Grujicic, M., Olson, G.B., 1985. Mobility of martensitic interfaces. Metall. Trans. A 16, 1713–1722.

Grujicic, M., Olson, G.B., Owen, W.S., 1985. Mobility of the beta-1-gamma-1′ martensitic interface in Cu–Al–Ni. Part 1 and 2. Metall. Trans. A 16, 1723–1744.

Haase, R., 1969. Thermodynamics of Irreversible Processes. Addison-Wesley, Reading, MA.

Hall, G.J., Govindjee, S., Sittner, P., Novak, V., 2007. Simulation of cubic to monoclinic-II transformations in a single crystal Cu–Al–Ni tube. Int. J. Plasticity 23 (1), 161–182.

Hill, R., 1984. On macroscopic effects of heterogeneity in elastoplastic media at finite strain. Math. Proc. Camb. Phil. Soc. 95 (3), 481–494.

Idesman, A.V., Levitas, V.I., Preston, D.L., Cho, J.-Y., 2005. Finite element simulations of martensitic phase transitions and microstructure based on strain softening model. J. Mech. Phys. Solids 53 (3), 495–523.

Kaganova, I., Roitburd, A.L., 1988. Equilibrium between elastically-interacting phases. Sov. Phys. JETP 67, 1173–1183.

Khachaturyan, A.G., Shatalov, G.A., 1969. Theory of macroscopic periodicity for phase transition in solid state. Sov. Phys. JETP 29, 557–561.

Khachaturyan, A.G., 1983. Theory of Structural Transformation in Solids. John Wiley and Sons, New York.

Kohn, R., 1991. The relaxation of a double-well energy. Continuum Mech. Thermodyn. 3, 193236.

Kruzik, M., Mielke, A., Roubicek, T., 2005. Modelling of microstructure and its evolution in shape-memory-alloy single-crystals, in particular in CuAlNi. Meccanica 40, 389–418.

Levitas, V.I., 1992. Thermomechanics of Phase Transformations and Inelastic Deformations in Microinhomogeneous Materials. Naukova Dumka, Kiev.

Levitas, V.I., 1995. The postulate of realizability: formulation and applications to post-bifurcation behavior and phase transitions in elastoplastic materials. Part I and II. Int. J. Eng. Sci. 33 (7), 921–970.

Levitas, V.I., 1996a. Large Deformation of Materials with Complex Rheological Properties at Normal and High Pressure. Nova Science Publishers, New York.

Levitas V.I., 1996b. Some Relations for Finite Inelastic Deformation of Microheterogeneous Materials with Moving Discontinuity Surfaces. In: Pineau, A., Zaoui, A. (Eds.), IUTAM Symposium on Micromechanics of Plasticity and Damage of Multiphase Materials. Proceedings of IUTAM Symposium. Paris, France, 1996, pp. 313–320.

Levitas, V.I., Stein, E., 1997. Simple micromechanical model of thermoelastic martensitic transformations. Mech. Res. Commun. 24, 309–318.

Levitas, V.I., 1998. Thermomechanical theory of martensitic phase transformations in inelastic materials. Int. J. Solids Struct. 35, 889–940.

Levitas, V.I., Idesman, A., Stein, E., 1999. Shape memory alloys: micromechanical modeling and numerical analysis of structures. Int. J. Intell. Mater. Syst. Struct. 10, 983–996.

Levitas, V.I., 2000. Structural changes without stable intermediate state in inelastic material. Part I and II. Int. J. Plasticity 16 (7-8), 805–849, 851–892.

Levitas, V.I., 2002. Phase field theory of martensitic transformation in inelastic materials. In: Khan et al. (Eds.), Proceedings of "Plasticity'02". Neat Press, Fulton, Maryland, pp. 195–197.

Levitas, V.I., Idesman, A.V., Preston, D., 2004. Microscale simulation of evolution of martensitic microstructure. Phys. Rev. Lett. 93 (10), 105701-1.

Levitas, V.I., Lee, D.-W., 2007. Athermal resistance to an interface motion in phase field theory of microstructure evolution. Phys. Rev. Lett. 99, 245701.

Levitas, V.I., Ozsoy, I.B., Preston, D.L., 2007. Interface reorientation during coherent phase transformations. Europhys. Lett. 78, 16003.

Levitas, V.I., Ozsoy, I.B., 2008. Micromechanical modeling of stress-induced phase transformations. Part 2. Computational algorithms and examples. Int. J. Plasticity, doi:10.1016/j.ijplas.2008.02.005.

Liu, Y., Xie, Z.L., 2003. Twinning and detwinning of ⟨011⟩ type II twin in shape memory alloy. Acta Mater. 51 (18), 5529–5543.

Lubliner, J., 1990. Plasticity Theory. Macmillan, New York.

Marketz, F., Fischer, F.D., 1996. Modelling the mechanical behavior of shape memory alloys under variant coalescence. Comput. Mater. Sci. 5 (1-3), 210–226.

Mielke, A., Theil, F., Levitas, V.I., 2002. A variational formulation of rate-independent phase transformations using an extremum principle. Arch. Ration. Mech. Anal. 162, 137–177.

Muller, C., Bruhns, O.T., 2006. A thermodynamic finite-strain model for pseudoelastic shape memory alloys. Int. J. Plasticity 22 (9), 1658–1682.

Olson, G.B., 1997. Computational design of hierarchically structured materials. Science 277 (5330), 1237–1242.

Olson, G.B., Cohen, M., 1972. A mechanism for the strain-induced nucleation of martensitic transformation. J. Less-Common Met. 28, 107.

Olson, G.B., Cohen, M., 1986. Dislocation theory of martensitic transformations. In: Nabarro, F.R.N. (Ed.), Dislocations in Solids, vol. 7, pp. 297–407.

Olson, G.B., Roytburd, A.L., 1995. Martensitic nucleation. In: Olson, G.B., Owen, W.S. (Eds.), Martensite, ASM International, Materials Park, OH, p. 149 (Chapter 9).

Pan, H., Thamburaja, P., Chau, F.S., 2007. Multi-axial behavior of shape-memory alloys undergoing martensitic reorientation and detwinning. Int. J. Plasticity 23 (4), 711–732.

Pankova, M.N., Roytburd, A.L., 1984. Orienting influence of applied stress on the martensitic transformation in alloys based on iron. Phys. Met. Metall. 58 (4), 81–90.

Petryk, H., 1998. Macroscopic rate-variables in solids undergoing phase transformation J. Mech. Phys. Solids 46, 873–894.

Popov, P., Lagoudas, D.C., 2007. 3-D constitutive model for shape memory alloys incorporating pseudoelasticity and detwinning of self-accommodated martensite. Int. J. Plasticity 23 (10-11), 1679–1720.

Rasmussen, K., Lookman, T., Saxena, A., Bishop, A.R., Albers, R.C., Shenoy, S.R., 2001. Three dimensional elastic compatibility and varieties of twins in martensites. Phys. Rev. Lett. 87, 055704.

Roitburd, A.L., 1974. Theory of formation of heterophase stucture under phase transformation in solid state. Sov. Phys. – Uspehi 17, 32–55.

Roitburd, A.L., Kosenko, N.S., 1976. Orientational dependence of the elastic energy of a plane interlayer in a system of coherent phases. Phys. Stat. Sol. A 35 (2), 735–746.

Roitburd, A.L., Kosenko, N.S., 1977. Elastic energy of a plate inclusion in an anisotropic elastic medium. Scripta Metall. 11 (12), 1039–1043.

Roitburd, A.L., 1983. Thermodynamics of phase formation in solids under external stresses. Sov. Phys. Crystall. 26, 628–633.

Roitburd, A.L., 1993. Elastic domains and polydomain phases in solids. Phase Transit. 45, 1–33.

Roytburd, A.L., Slutsker, J., 1997. Thermodynamic hysteresis of phase transformation in solids. Physica B 233 (4), 390–396.

Roytburd, A.L., Slutsker, J., 2001. Deformation of adaptive materials, Part III: deformation of crystals with polytwin product phases. J. Mech. Phys. Solids 49 (8), 1795–1822.

Salje, E.K.H., 1990. Phase Transitions in Ferroelastic and Co-Elastic Crystals. Cambridge University Press, New York.

Saxena, A., Wu, Y., Lookman, T., Shenoy, S., Bishop, A., 1997. Hierarchical pattern formation in elastic materials. Phys. A: Stat. Theoret. Phys. 239 (13), 18–34.

Shaw, J.A., 2000. Simulation of localized thermo-mechanical behaviour in a NiTi shape memory alloy. Int. J. Plasticity 16 (5), 541–562.

Stupkiewicz, S., Petryk, H., 2002. Modelling of laminated microstructures in stress-induced martensitic transformations. J. Mech. Phys. Solids 50 (11), 2303–2331.

Sun, Q.P., Hwang, K.C., 1993. Micromechanics modelling for the constitutive behavior of polycrystalline shape memory alloys. I. Derivation of general relations. J. Mech. Phys. Solids (1), 1.

Thamburaja, P., 2005. Constitutive equations for martensitic reorientation and detwinning in shape-memory alloys. J. Mech. Phys. Solids (4), , 825–85.

Wang, Y., Khachaturyan, A., 1997. Three-dimensional field model and computer modeling of martensitic transformations. Acta Mater. 45 (2), 759–773.

Wayman, C.M., 1964. Introduction to the Crystallography of Martensitic Transformation. Springer, New York.

Wechsler, M.S., Lieberman, D.S., Read, T.A., 1953. On the theory of the formation of martensite. Trans. AIME 197, 1503–1515.

Zheng, Q.S., Liu, Y., 2002. Prediction of the detwinning anisotropy in textured NiTi shape memory alloy. Phil. Mag. A 82, 665–683.

Ziegler, H., 1977. An Introduction to Thermomechanics. North-Holland, Amsterdam.